TAMPEREEN TEKNILLINEN YLIOPISTO
TAMPERE UNIVERSITY OF TECHNOLOGY

HATAI JONGPRASITKUL

STUDIES ON MICROPOROUS BIODEGRADABLE POLYMER FILMS

Master of Science Thesis

Examiner: Professor, Dr Sci Minna Kellomäki,
Teresa Rebelo Calejo, PhD
Examiner and topic approved by
The Council meeting of the Faculty of Natural Sciences on 6th May 2015

ABSTRACT

TAMPERE UNIVERSITY OF TECHNOLOGY
Master's degree program in Biomedical Engineering
HATAI JONGPRASITKUL: STUDIES ON MICROPOROUS BIODEGRADABLE POLYMER FILMS
Master of Science thesis, 70 pages
May 2015
Major: Biomaterial
Examiner: Professor, Dr Sci Minna Kellomäki, Teresa Rebelo Calejo PhD
Key words: Polymer films, Breath figure method, Honeycomb films, Porous films

Breath figure method or BF was the main technique in this project to create polymer films with porous structure for RPE cell culture due to the method being simple and inexpensive and enabling the formation of evenly porous honeycomb-like pores in polymer films. Various parameters of BF method leading to different set of morphologies in pore size, pore number and order. By doing so, it was the aim of this project to develop porous films based on low toxicity components and can be applied in tissue engineering applications.

The project is mainly divided into three parts: (1) preparation of polymer films (2) characterization of polymer films. The procedure for creating porous polylactide (PLA) and polycaprolactone (PCL) films was done by varying different parameters to acquire the honeycomb-like structure. The parameters considered for film preparation were mainly the type of polymer (PLA and PCL), polymer concentration, solvent (ethyl acetate and THF), surfactant (Tween80 and PVA), surfactant concentration and percentage of relative humidity in the environment**.** The structural features such as pore sizes, pore distribution, and pore arrangement were investigated via optical microscopy and atomic force microscopy. Contact angle measurement was used to measure the wettability of the surface of the films. Film thickness was measured using a micrometre.

The results showed that various parameters (polymer type, polymer concentration, solvent, surfactant and humidity) could affect the structural characteristics of thin films such as homogeneity of films, pore size, pore distribution, wettability and thickness. Honeycomb pore films could be produced from PLA solution (26 mg/ml concentration) and ethyl acetate with Tween 80 under humid environment (85-95 of RH %), which produced a good arrangement of pores (honeycomb-like pattern), and pore sizes in the range 2-4 µm.

It was concluded that increasing concentration of polymer could reduce pore sizes and increase the film thickness accordingly. Adding an amphiphilic component or surfactant could reduce pore size also. Moreover, contact angle decreased when films were prepared in the presence of surfactant compared to films prepared without surfactant. Honeycomb films with minimal toxicity were obtained in this work, but it was only in small area and the improvement should be carried out in near future.

PREFACE

This work was carried out in the Biomaterials and Tissue Engineering research group, Department of Electronics and Communications Engineering at Tampere University of Technology and the project was also connected to BioMediTech, a joint institute between: Tampere University of Technology and University of Tampere. This thesis focuses on preparation of polymer films as a possible treatment for Age-related macular degeneration as retinal pigment epithelium transplantation in the future.

This thesis was done under the guidance and advice of Professor, Dr Tech Minna Kellomäki and Teresa Rebelo Calejo PhD. They gave me an interesting topic to carry on. Furthermore, I would like to express my grateful especially my supervisor Teresa Rebelo Calejo PhD who taught me many things about the laboratory including the basic to the advanced knowledge until I finished the work and also helped me to finalize the writing part of my Master thesis (without hesitation to help me).

Moreover, I would like to thank Suvi Heinämäki because she always gave me useful instructions about the laboratory and she took care of my hand injury when I had the accidence during the work. Also, I am grateful to M.Sc. Maiju Hiltunen for her advice about the AFM imaging. In addition, I want to say thank you to Hemmilä Samu for teaching water contact angle measurements.

I also appreciate all of my friends who worked with me during the summer and gave me a positive attitude about the Finnish culture.

Finally, I would like to thank my family in Thailand, who supported me during the life in Finland. They always encouraged me to study abroad when I was in Thailand.

Hatai Jongprasitkul

TABLE OF CONTENTS

TERMS AND DEFINITIONS

AFM	Atomic force microscope
AMD	Age-related macular degeneration
BF	Breath figure method
CAP	co-carboxyhexyl acrylamide
CNS	Central nervous system
CNVMs	Choroid neovascular membranes
CS	Carbon disulfide
DR	Diabetic retinopathy
ESC	Embryonic stem cells
EOG	Electrooculography
hESCs	Human embryonic stem cells
ICM	Intra cellular matrix
PCL	Polycaprolactone
PDO	Polydioxanone
PDMS	Poly(dimethylsiloxane)
PE	Polyethylene
PGA	Poly(glycolic acid)
PGMA	Poly(glyceryl methacrylate)
PLA	Poly(lactic acid)
PLGA	Poly(lactic-co-glycolic acid)
PS	Polystyrene
PTFE	Polytetrafluoroethylene
PU	Polyurethane
PVA	Polyvinylalcohol
RH%	Percentage of relative humidity
RP	Retinitis pigmentosa
RPE	Retinal pigment epithelium
ROP	Retinopathy of prematurity
SD	Standard deviation
SEM	Scanning electron microscope
THF	Tetrahydrofuran
MAI	Poly[methyl acrylate-co-(2-hydroxyethyl acrylate)]
VEGF	Vascular endothelial growth factor
w/v	Mass concentration (weight/volume)

1. INTRODUCTION

Age-related macular degeneration or AMD is one illness that leads to vision loss or even blindness in elderly people. In AMD, cells in the retinal pigment epithelium or RPE, which plays role in the neurosensory retina, becomes degenerated or die affecting the photoreceptor cells. Various studies show that there is no obvious treatment option for the disease.

The aim of this study was to investigate new porous materials for RPE cell transplantation, having in mind the use of low toxicity components, thereby improving the biocompatibility of the material. In addition, it was considered important that pores sizes were in the range 1-4 μm because smaller pores could reduce the permeability. In this case, the material requirement should be permeable, which could allow the nutrients, oxygen and waste products to go through the membrane after transplantation ensuring the cell survival. Bigger pores would make the cells go through the membrane. Moreover, the thickness of polymer films should be around 2-4 μm according to the Bruch's membrane where the RPE cells lie on the retina.

Polymer films with porous structure are widely used in various applications such as microelectronics, biotechnology, photonics and scaffold for synthesis of composite materials [1]. There are many successful methods, which have been developed in order to fit the need of their purposes including controlling pore sizes in both micro and nanoscale embedded on the film surface. In particular, the breath figure method is one of the most widely used techniques to achieve ordered porous polymer films. The basic mechanism of breath figure method relies on the self-assembling of water droplets from the moist air in the environment because the water droplets in the air will condense on the polymer solution creating the holes. After the water droplets evaporate entirely, they will leave the porous structure on the polymer surface.

Honeycomb structure has been invented to rearrange the polymer properties such as space area, attachment ability structural stability, mechanical strength, density and permeability [2]. Breath figure method is also the simple, quick, and inexpensive, thus, it has been implemented for preparing organized honeycomb porous structures on the film. In this project, the polymer solution in certain solvent with or without surfactant was cast in the Petri dish under humid environment and prepared with breath figure method to

obtain porous film as a result. A number of parameters were varied and investigated in this study such as type of polymer, solution concentration, hydrophilic property, different pore arrangement, solvent and surfactant. The observation of the polymer films in this work revealed pore sizes, pore distribution, film thickness, contact angle and the growth of RPE cell culture.

2. THE EYE

The eye is a complex and highly evolved organ in human body having heavy importance for life that gives vision by detecting the light and converting to electro-chemical drive in neurons or optic nerve that allow us to see the object which is processed by the brain into a visual perception [3]. Eyeballs are located in the orbital bone socket in front of the skull surrounded by the upper skin layer, fat tissue, nerves, extraocular muscles, and blood vessels that supply the eye with nutrients [4]. The eye consists of three main layers: sclera, uvea and retina. The outer layer of the eye is made up for protection and surrounded by sclera and cornea, it is also called corneo-scleral shell [5]. In the anterior segment of middle layer forms the iris and ciliary body. The anterior components are designed to receive the light into the eye ball and then focus or refract the light to project on the retina. The posterior segment consists of retina which is composed of photoreceptors and pigment epithelium, located in the innermost layer of the eye. The posterior components are designed to detect the light coming from the anterior segment and transmit to the brain by electro-chemical impulses [6].

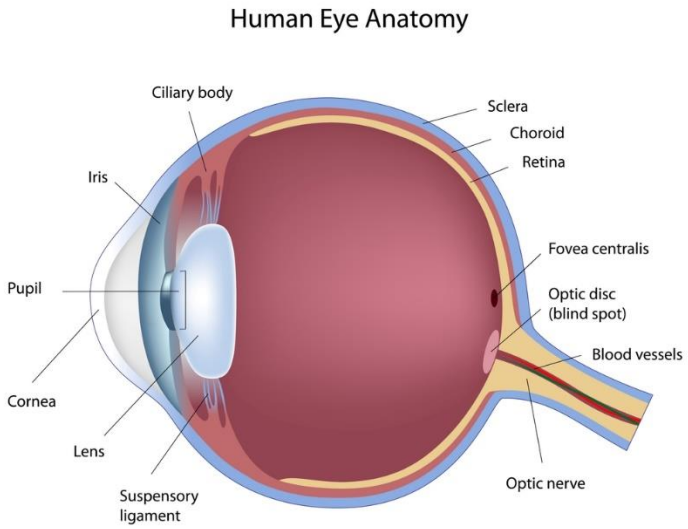

Figure 1. Simplified structure of human eyes [7].

2.1 Retina

The retina can be explained as a transducer that converts electromagnetic energy (light) to electrical form in order to transmit and perform an action potential through the fibers of the optic nerve [8]. The retina is a thin-sensitive tissue layer located in the inner surface of the posterior segment to receive the light from the opening segment in the front, which is nourished by various blood vessels [9]. It is surrounded by pigment epithelium that contains melanin, which helps to reduce backscatter of the light as well as maintenance of photoreceptor cells [10]. These well-organized structures are called nuclear layer and separated by two other layers containing synapses made by axons and dendrites. Retina is one part of central nervous system (CNS) where the optic nerves are attached directly to the brain and assumed that it is the visualized of CNS system [11]. The central region of the retina is called fovea [12]. The major components of the retina are the retinal pigment epithelium, photoreceptors, the ganglion cells, and the glial cells.

Basically, the retina is composed of two types of photoreceptors, rod and cone cells which have different function. There are approximately 125 million rod cells in the human retina [13]. The rod cells are very sensitive especially the dimmed light and mainly responsible for night vision, but they cannot distinguish the color [14]. Cone cells are responsible for color detection and require higher levels of light to generate signal.

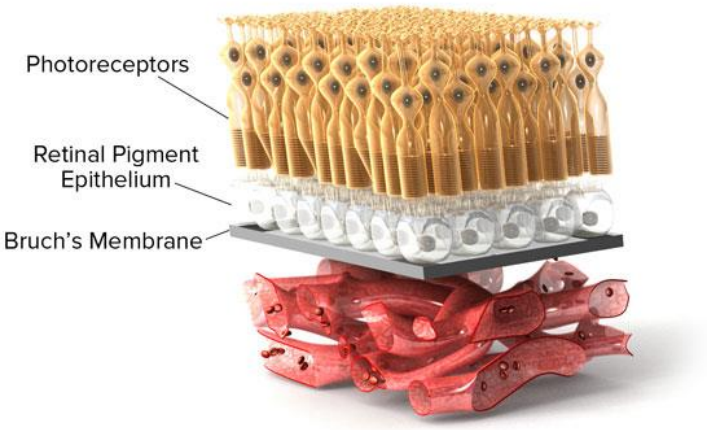

Figure 2 The layer of retina [15]

2.1.1 Retinal pigment epithelium (RPE)

Retinal pigment epithelium is a sensory tissue made up from a pigmented cell layer attached to the choroid and retinal visual cells [16]. It is a monolayer that has a cuboidal shape in cross section and high pigmentation, and it lies on the Bruch's membrane between the neural retina and the choriocapillaries. In normal adult humans, the retina contains around 3.5 million of retinal pigment epithelium cells [17]. It has the main role to support photoreceptor function in order to absorb especially scattered light to improve quality of the optical system. Moreover, the retinal pigment epithelium also plays a role in supplying nutrients to the photoreceptors and it also controls the ion homeostasis and eliminates water from retinal tissue [18] [19].

RPE cells also maintain the various photoreceptor functions such as phagocytosis of photoreceptor outer segments, protection against reactive oxygen species, synthesis of vitamin-A metabolites (retinoid recycling) and maintaining the retina blood barrier formed by the capillary endothelium of the intrinsic retinal vasculature, which are suitable for maintaining the visual function. Retina has high metabolic activities that can produce oxygen especially in macula part for RPE cells [20]. The pigment or melanin in RPE cells can provide the absorption of the excessive and scattered light in the eyes. The human body firstly develops RPE which later become pigmented, after that melanogenesis continues for entire life , but the RPE cells in the older age can be broken down and appear to be less pigmented [21].

However, RPE cells are not photoreceptors and they cannot respond directly to the emitting light, but they can induce the electrical activities of the apical and basal membranes that can generate the transepithelial voltage or the standing potential. When the photoreceptor contacts the incoming light and response, the concentration of potassium decreases for a certain period in seconds in the subneural retinal space. Then, the RPE cells respond by hyperpolarizing. Light activation of photoreceptors can be interpreted in clinical way to observe the Electrooculography (EOG) wave of patients who suffer the abnormal activities such as cystic fibrosis [22]. For the regeneration process of RPE cells, RPE cells can sometimes repair themselves locally. For example as a response to, the damage of RPE from burn or laser beam, the cells will begin to divide surrounding the burn and small cells fill the defect to form a new blood-retinal barrier within 1–2 weeks [23].

In retinitis pigmentosa, the RPE cells accumulate into the injured neural retina and then surround the vessels to contribute to the characteristic bone spicule appearance. An excessive RPE growth can cause the duplicated layers of RPE cells and RPE scarring, which may be part of a macular degenerative process [23].

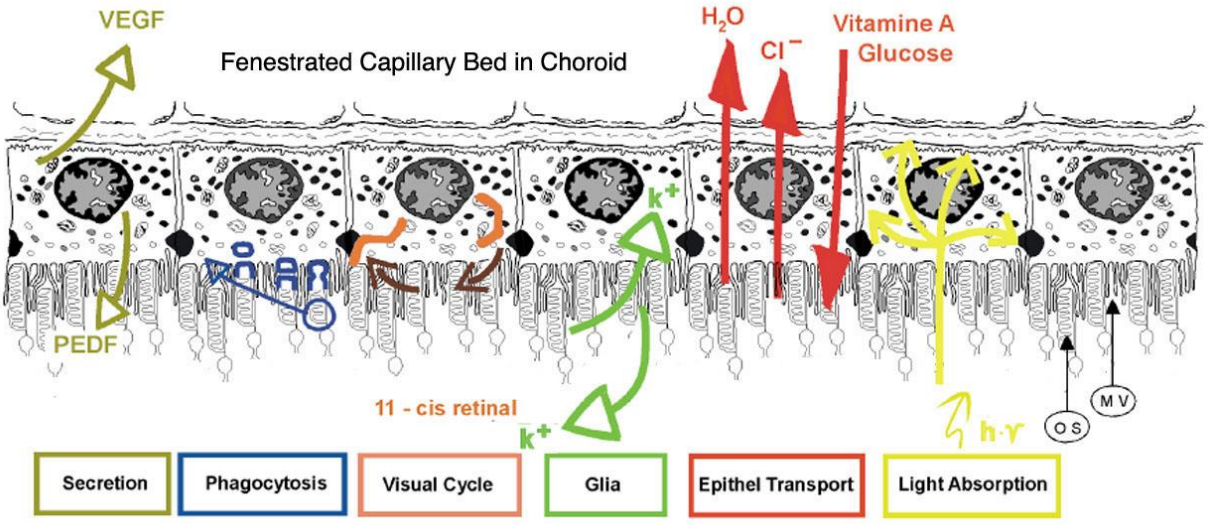

Figure 3 Simplified main functions of RPE [24]

2.1.2 Bruch's membrane

Bruch's membrane is a thin membrane composed with five layers – the basement membrane, inner collagen fibre layer, elastic fibre sheet, collagen fibre layer and the basement membrane of the capillary endothelial cells of the choriocapillaris [25]. The membrane is located between the RPE layer and the size is around 2-4 μm in thickness, but it has very good mechanical properties, mostly due to the presence of collagen and elastin [26]. The membrane itself extends anterior to the ora serrata and forward to retinal epithelium of the ciliary body, which can be activated only by the optic nerve. The Bruch's membrane serves as the substratum of the RPE, which is a major clinical problem in age-related macular degeneration (AMD) and other choroid disease [27].

3. OPHTHALMOLOGY

3.1 Retinal disorder

Degenerative retinal disorder is a common condition found in aging population and can be serious problem if untreated, possibly causing irreversible blindness. The number of patients who suffer from this disease, has been increasing for the last 80 years in developed countries [28]. Degenerative disease affects the photoreceptors in the retina and leads to progressive photoreceptor cell impairment. The central nervous system (CNS) loses its ability to regenerate these damage neurons, consequently the vision loss cannot be prevented [29]. The most common retinal diseases are age related macular degeneration (AMD), retinitis pigmentosa (RP), diabetic retinopathy (DR) and retinopathy of prematurity (ROP).

3.1.1 Age related macular degeneration (AMD)

Age related macular degeneration is a complex multifactorial disease that can cause blindness and that commonly occurs in elderly people over 60 years old. Over 30 million people worldwide suffer from AMD, and half of this group acquire severe blindness. AMD causes the damage of the macular located in the center of retina, which causes blurred vision [30]. Progressively, blurred vision grows larger and consequently develops a blank spot in the central vision. Moreover, the object may appear to have a different shape or color in each of the eyes or may appear smaller. AMD basically can be divided into two categories: neovascular (wet) or atrophic (dry) (Figure 4). The symptoms of AMD usually progress from the dry form into the wet one [31]. The wet form also called called neovascular or exudative AMD can lead to visual loss as a result of choroidal neovascularisation. In this case, the new vessels overgrow and invade the retina, which can cause sub-RPE or subretinal haemorrhages, or fluid accumulation in or below the layers of the retina [32]. Around 80% of wet AMD patients suffer from severe visual loss or legal blindness [32]. The AMD cannot be detected clearly before the age around 55 years old. The trail of AMD can be indicated by the pigment disruption and formation of drusen in RPE.

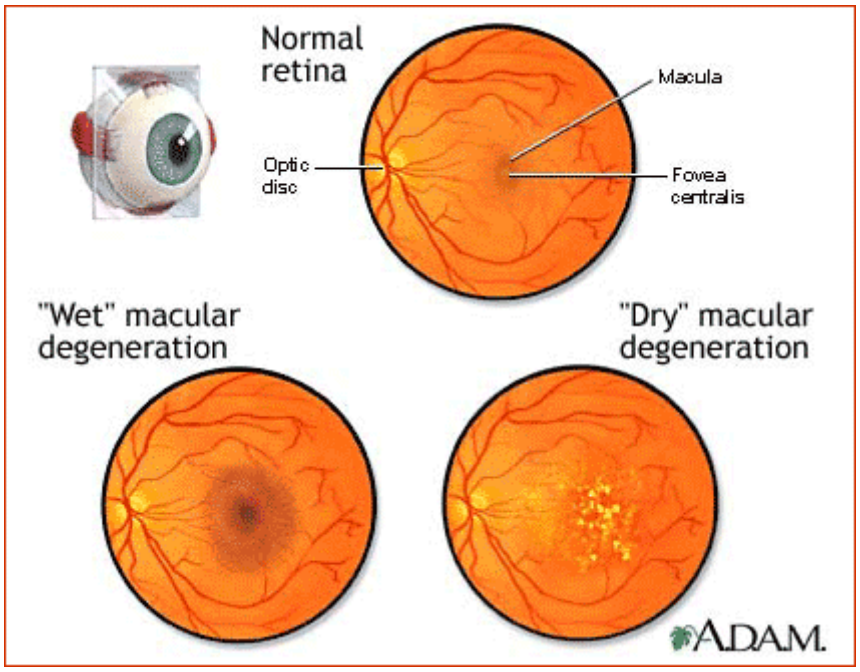

Figure 4 Different types of AMD compared normal retina [33]

3.1.1.1 Treatment

The treatment for AMD has focused mostly on the wet form due to its rapid progression and debilitating nature. The treatment includes the intraocular injection of anti-vascular endothelial growth factor (VEGF) drugs and photodynamic therapy [34]. The angiostatic steroids (triamcinolone acetonide and anecortave acetate) are effective in blocking neovascular membranes from forming by inhibiting angiogenesis, however these therapies have dangerous side effects including elevated intraocular pressure and cataract formation [35]. The effectiveness of anti-inflammatory treatments in halting pathologic angiogenesis supports the theory that the pathologic growth of blood vessels in wet AMD is associated with inflammation [36]. Without treatment, patients will severely lose their central vision, which can affect the quality of life and ability of daily living.

However, there is no complete cure available for AMD [37]. Current therapies focus on preventing and slowing down the progressions of AMD, so far, no effective treatments have been developed yet.

- *Prevention*

Vitamin consumption or the combination of minerals and antioxidants such as 15 mg of beta-carotene; 500 mg of vitamin C; 400 IU of vitamin E; 80 mg of zinc; and 2 mg of copper to prevent zinc-induced anaemia have been shown to reduce the progression of high-risk AMD patients by 25% [38]. In addition, the clinical trial AREDS-2 was introduced in 2006 and aimed at assessing the effect of DHA/EPA (omega-3 fatty acids) or lutein and zeaxanthin (macular xanthophylls), in slowing down the advance of AMD in patients. In some cases, Beta carotene has been used widely, but the studies showed that it causes a higher risk of lung cancer in current and former smokers, so it was planned to replace with lutein and zeaxanthin in the future [39].

Some researchers revealed that the current possible treatment of macular degeneration is lutein [33]. However, several factors that cannot be controlled such as gender, age and individual lifestyle. Dr. Johanna Seddon, currently of the Harvard University School of Medicine, had a study published that examined the effects of the consumption of certain carotenoids and the prevalence of AMD [40]. This study found that when people took 6mg of lutein each day, this led to a 43 percent lower chance of contracting AMD.

3.1.2 Retinitis pigmentosa (RP)

Retinitis pigmentosa is a genetic disease which is categorized by the progressive photoreceptor cell death. Over 1.5 million people suffer from this condition in worldwide [41]. Basically, RP leads to progressive death of photoreceptors, particularly rod cells. The symptoms are difficult night vision and defected visual field. Moreover, complications such as diverse chromosomal, metabolic and morphology features, can be determined genetically [42]. It is difficult to treat RP as well as dry AMD, in which the current treatment is only to slow down the progression of disease. Gene therapy is another potential therapeutic option that has gained support from researchers recently [43].

4. RETINAL TREATMENT USING BIOMATERIALS

4.1 Possible materials for retinal treatment

Several materials and designs have been proposed for manufacturing the products of retinal treatment including permanent implants and absorbable devices. However, the degradable devices present a high number of problems and less advantages in comparison with the permanent ones [44]. The materials are categorized into polymers, absorbable implants and natural materials, which will be discussed the detail below.

Polymer

Polyethylene (PE)

In the first stage, polyvivol has been tested and presented unsatisfying results in the mid-1950s, in which the polyvivol produced a harmful reaction in the ocular tissues that was thus considered not suitable for clinical applications. After that, polyethylene was proposed because it is easy to manufacture into different shapes. PE is a hard and rigid material, which can cause erosion of the underlying sclera and choroid [45].

Polytetrafluoroethylene (PTFE)

PTFE was tested in 1960s by Wolter *et al* [46], meanwhile another report from Deodati et al [47] showed the adverse result that the Teflon provided the same complication as PE. Moreover, the porous PTFE has been invented in the form of buckling band or coating on silicone implants with various outcomes, which could be an alternative materials and should be further studied in term of performance and *in vivo* effects [45].

Poly(glyceryl methacrylate) (PGMA)

PGMA has been used as a potential hydrogel since 1970 and it has shown better results than silicone implants, still being used today. PGMA has however shown the lack of tensile strength when swollen [45].

Poly[methyl acrylate-co-(2-hydroxyethyl acrylate)] (MAI)

MAI is also used as softer hydrogels, which have shown a lower risk of infection than any materials used in the past around 1990 [45]. MAI is commercially sold as Migrel. It is one of the best materials for scleral buckling and it can last for more than 10 years. However, MAI has been associated with the risk of severe long-term complications such as persistent pain and foreign body sensation and need to be re-operation for the removal of the implants [48].

Absorbable implants

Absorbable implants of degradable materials are used as to replace the scar tissue in the normal course of tissue turnover, which can take process around few weeks or a year to achieve depending on the degradation rate of the chosen material [49]. The absorbable implants have being studied in the experiment such as rabbits. The absorbable have a problem that lack of ability to last long in the host. In the first era, biological materials were used and could not meet the desired results, which made the synthetic polymers more promising options to fulfill the clinical outcomes in vivo, which included poly(glycolic acid) (PGA), poly(lactic acid) (PLA), PGA/PLA composites, polydioxanone (PDO) and polyurethane (PU) [45]. They provide minimal adverse effects, controllable, predictable absorption kinetics and they can also be shaped easily [48].

4.2 Tissue engineering for retina

In order to improve the regeneration of retinal tissue, retinal transplantation has been considered a very promising therapeutic option, using a variety of cell types including embryonic stem cells, fetal cells, progenitor cells and induced pluripotent stem cells [50]. The treatment can be classified according to 2 approaches: to restore the photoreceptors and to replace the retinal pigment epithelium [51]. Embryonic stem cells (ESC), are derived from the inner cell mass of the blastocyst [52]. They give rise to the body's three germ layers (endoderm, mesoderm, and ectoderm) with unlimited self-renewal and then, when the cells are ready, the ESC has an enough potential to differentiate into any of the body's over 200 cell types [53]. The transplantation of retinal pigment epithelial cells has been introduced around two decades ago, with a positive outcome in both surgical and clinical studies [54].

Autologous and allogeneic transplantation

In present, the autologous RPE is implemented in clinical studies because the cells cannot last long in elderly patients due to the transplants need immunosuppressive therapies. Moreover, it is difficult to collect sufficient number of autologous RPE cells for wide-scale clinical use, despite it led to clinical benefits to some patients. Because of these issues, stem-cell therapy is also focused to create RPE cell lines for transplantation [55]. RPE transplantation has been reported as a successful method to recover patients' vision from blindness and the success of transplantation depends on the origin of RPE cells. In autologous transplantation, the cells are taken from the same patient (own eye),

while in the allogeneic transplantation, foreign cells are used [56]. One example of RPE transplantation for the treatment of wet AMD, includes a pars plana vitrectomy and two retinotomies, where the surgical procedure begins with the removal of the damaged subfoveal membrane and then the surgeon will remove RPE cells in different regions of the retina. After that, the harvested RPE cells will be deposited into subretina space [57]. Both allogeneic and autologous transplantation have disadvantages, such as the possibility of rejection by the host or the autologous RPE may already malfunction by current disease [56].

Possible polymers for tissue engineering

Polymers can constitute scaffold materials for retinal tissue engineering, in which the materials themselves should have biocompatibility with the eyes, causing no immune response in the subretinal space. They should have also good mechanical properties as well as flexibility to tolerate surgical manipulation and keep the surrounding tissues intact [58]. The materials should imitate the Young's modulus value of the sensory retina. Moreover, the materials should have good permeability or porous structure in order to ensure diffusion of nutrients and other substances from the choriocapillaris. Biodegradable properties are also taken into account to slow disintegrate through hydrolysis without altering retina's extracellular milieu. The material choices that are considered such as collagen, PLLA, PLGA, gelatin, poly(glycerolsebacate), poly(methylacrylate/methacrykamide), poly(dimethylsiloxane)(PDMS) and polyurethanes as well as many others, which are good for scaffold materials for RPE cell transplantation [59].

4.2.1 Human embryonic stem cells (hESCs)

Human embryonic stem cells are mainly pluripotent cells that have capability to differentiate into 3 germ layers. These cells have been extensively investigated due to their importance on clinical application for cell replacement technology [60]. The first stable hESC lines were derived in the USA by Thomson in 1998 [61]. In 2001, BresaGen's hESC lines were announced and qualified for funding under the criteria outlined by President Bush. Basically, hESC cells will differentiate into RPE cells after six to eight weeks, which investigated this theory in the cell culture in 2006 and called the theory of neural induction. For the cell culture protocol, the hESCs usually is cultured in the cell-cultured plate and isolated from the intracellular matrix (ICM) of a four to five days of embryo [62].

Cell-material interactions

Cell-material interactions are very important in tissue engineering because they can explain the differences in cell behavior in culture conditions. In current research, 3D-coating materials have been studied largely for cell-material interactions, which are commonly used for bone applications. However, there is no the optimal method for coating because the material depends on the cell lines and culture conditions [63].

Protein adsorption

Stem cells are grown in cell culture of rigid polystyrene plastic bottles *in vitro*, at various culture conditions. Cells anchor to ECM proteins by discrete attachments in the microenvironment. Cell culture proteins such as fibronectin, laminin and collagen, usually interact with specific receptors on the surfaces. The adhesion between the cells and protein is carried out through by integrins (The integrins are members of the family of cellular adhesion molecules that are expressed by several cell types) [64].

Characteristics of materials

The surface properties of the material affect the cell attachment directly. The cell adhesion can be better on hydrophilic than on hydrophobic surfaces because the surface needs to be wet to create an appropriate support for cell adhesion. Several resorbable polymers in tissue engineering are hydrophilic or require surface modification or wetting before the procedure. Moreover, the roughness of the surface can affect the cell attachment as well, which they create more spaces ,but can interfere with wetting of hydrophobic surfaces due to the reduction of the exchange between the surface and the solution [65].

5. POROUS FILMS

Porous materials have high surface-to-mass ratio with a high absorption properties. They can be used in various applications such as a catalyst or exchanger, depending on the type of material and their composition [66]. In medical applications, the porous materials are considered advantages because they have unique properties such as high surface-to-mass ratio along with a high absorption capacity of the molecules. This makes them useful in many medical applications including thin films, drug delivery, cell culture, and catalyst. In general, the porous materials can be classified in different types depending on their materials, fabrication techniques and set of pores (pore sizes, shape and pattern) [67]. Several materials with a specific surface area and morphology such as polymer, porous glasses, silica gels, and activated carbon have been used to produce porous film. Thin films can be prepared in different ways, for instance, mold application, colloidal lithography, electro-spinning and various techniques. However, the advance fabrication methods for porous films are expensive and slow [68]. So, the solvent casting technique (breath figure method) was the main focus of this work because it is a simple, faster and cheaper technique.

Porous films can be substrates for retinal pigment epithelium cells (RPE cells). Thin porous films can be used as carries for transplantation of RPE cells and replacement of RPE cells. Alternatively, other authors have been studying the injection of suspensions into sub retinal space and also the transplantation method with and without collagen support [69]. The use of polymer films as porous material is established such as PLA, poly(lactic-co-glycolic acid) (PLGA) or other biodegradable polymers. They are biocompatible, biodegradable and have been implemented for tissue engineering purposes. Moreover, RPE cells have been shown to attach to thin films of PLGA *in vitro* in some studies [70]. And they can be applied with certain growth factors or drugs, where the film plays a roles as a drug delivery system (short-term) [71].

5.1 Honeycomb films

The hive of the honeybee is usually formed by natural wax, which is secreted from their own bodies to build the honeycomb. It is a perfect hexagonal geometrical structure (Figure 5), which has amazing properties such as large space area, good mechanical properties to maintain the overall structure, high mechanical strength, low density and various functions [72]. Many researchers have been trying to investigate the process of forming honeycomb structure in biomaterial for artificial materials [73]. In particular, the mimicking of natural structure of honeycombs can lead to the new design of materials with multiple application in engineering and biology.

There are many methods to construct the pattern of honeycomb materials with high control of pore features. However, the procedures are in general expensive, complicated and multiple steps are required to complete the ordered honeycomb structures. In addition, the structure can be damaged because of the template removal after the final step. In 1994, an article described the procedure by which the condensation of water droplets form a honeycomb pattern on the materials, which was called breath figure method (BF) [74].

Figure 5 Example photos of honeybee with the combs from the top view [75].

6. BREATH FIGURE METHOD

6.1 Introduction

Breath figure or BF is the method by which the water droplets are used to create an array at the surface of a cold substrate. It has been investigated in the past two decades as a means to generate ordered micro and nonporous structures in polymeric materials [76]. The technique is used in the tissue engineering fabrication of scaffolds, where big pores are required for the penetration of cells. In 1994, Francois et al [77], discovered the formation of an ordered porous film when the star-shape polystyrene (PS) in carbon disulfide (CS) was applied to a flow of moist air. The micro pores were arranged in a hexagonal way after the solution dried, forming structure that resembled a honeycomb.

The BF technique is being investigated nowadays in order to produce porous films with using a simple, cheap and fast method. The BF method was developed in order to create ordered pores on the film with precise control of pore size (from nanometer to micrometers) and distance between pores. The alternative methods for the formation of porous films are solvent casting, freeze-drying, salt-leaching, fiber bonding and electro-spinning, but the pores are not organized and homogeneous in size. The number of condensed droplets at the surface and the size of water droplets can also vary according to the solid surface properties or the type of materials, and many studies revealed the various parameters leading to different set of morphologies in pore size, pore number and order.

6.2 Mechanism of BFs

Currently, BF is a promising way to create a regular pattern of pores. Basically, there are three main stages in the BF process (Figure 6). First of all, the solvent begins to evaporate in moist environment and the water droplets in the air condense on the polymer solution simultaneously. After that, the water droplets grow on the solution surface [78]. The droplets are then nucleated and grow on the small surface area, forming ordered templates.

When the surface is covered by the water droplets in the entire area, then the water droplets and the solvent evaporate and leave the arrangement of pores on the surface organized into a honeycomb structure. The surface structure can be observed by the microscope.

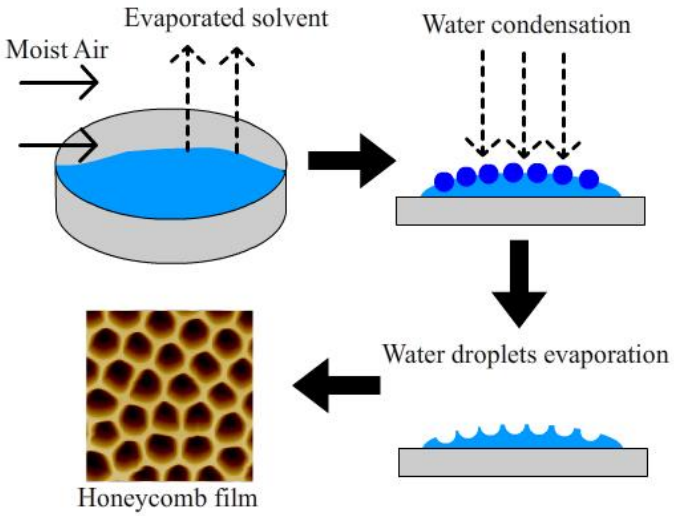

Figure 6 The simplified scheme of breath figure method (BF).

6.3 Polymers used in the production of porous films by the BF method

The research from Francois et al in 1991 [79], revealed that various structures of polymers such as star and rod-coil polymers can form the honeycomb films via BF method. In the beginning of this study, different parameters such as polymer types, solvents and other substrates were investigated to acquire all patterns of honeycomb films. The research indicated that specific combinations/conditions led to the formation of pores via the imprint of the water droplets. Some examples of polymers used in the preparation of honeycomb films are described and classified in Table1.

Table 1 Different polymers used in the production of honeycomb films by the BF method

Polymer architecture	**Example of polymers**	**Conditions**	**Observation**	**References**
Starlike and graft polymer	Polystyrene(PS), co-grafting styrene and divinylbenzene into a microgel	CS_2 as solvent, Polymer concentration, Molecular weight blending glucose- and carboxy-terminated PS, 85% of humidity, air velocity	Pore sizes: 150 nm-1µm	[80] [81] [82] [83]
Block copolymer	polystyrene-co-poly(2,3,4,5,6-pentafluoro styrene) (PS-co-PPFS)	CS_2, $CHCl_3$, CH_2Cl_2 as solvent, copolymer concentration, 85% of humidity	Less ordered pore structure compared to Starlike and graft polymer	[84]
Amphiphillic polymer	Amphiphillic polymers and polymers with polar groups at the terminal chain, Polystyrene(PS)	Phospholipids as surfactant	The surfactant can stabilize the condensing water droplets preventing from coalescence,	[85] [86] [87]

6.4 Solvent

The solvents play role to dissolve the polymer particles and also accelerate the porous structure of the film in the high humidity environment. Many solvents can be considered in the BF method to dissolve the polymer such as benzene, toluene, chloroform, THF, ethyl acetate, and dichloromethane. Each type of solvent has different drying properties such as drying-time and boiling point, which can affect the pore size. For example, when using toluene as solvent, lower pressure is needed in order to obtain the porous structure on the surface. In many studies, it is shown that THF and chloroform are better than any other solvents in both dissolvability and water-solubility [88].

In the BF method, the surface of the solution begins to dry and the water in the environment condenses at the same time. The water droplets on the surface cause the formation of shallow pores. When the density of the solvent is lower than the density of water, the water droplets will sink into the solution and begin to form small holes in the surface and increase the pore sizes, which will depend on the solvents and RH% in the environment.

The alternative way to decide the solvent for polymer films is to consider the following parameters: high vapor pressure, low boiling point, low solubility in water and preferentially higher density than water. According to the table, it can be seen that chloroform is the best solvent to form a highly ordered structure of honeycomb films prepared by BF method.

Table 2 The different solvents used in the BF method [89]

	Chloroform	**Dichloromethane**	**Carbon disulfide**	**Toluene**	**THF**	**Pentane**	**Diethyl ether**	**Ethyl acetate**
Density (g/cm^3)	1.48	1.32	1.26	0.86	0.89	0.62	0.71	0.90
Vapor pressure (KPa)	21.3	46.5	39.7	2.9	21.6	56.8	58.6	9.7
Solubility in water (g/L)	8.2	20	2.9	0.5	Miscible	0.4	69	87
Boiling point (°C)	61	39	46	110	65	36	34	77

6.5 Effect of surfactant

Surfactants are a main key to reduce surface and interfacial tension of water dissolved in solution as well as orientating at the surface. The chemical structure of a surfactant is basically divided into water-liking or hydrophilic and water-hating or hydrophobic. These molecules are amphiphilic, in which the hydrophobic parts are removed from the aqueous environment as shown in Figure 7. The surfactant molecules will replace water molecules on the surface, which can reduce the bonds between water molecules and lead to reduce the surface tension [90]. Surfactants are described into many different types depending on their charge characteristics, for example, they can be anionic, cationic, non-ionic or zwitterionic (ampholytic).

In the BF method, the surfactant stabilizes the water droplets in the polymer solution. As a result, the surfactant can maintain the formation of a water-template on the surface that forms the well-organized honeycomb pattern film. However, the toxicity and biodegradability have to be taken into account partially when medical applications are envisioned.

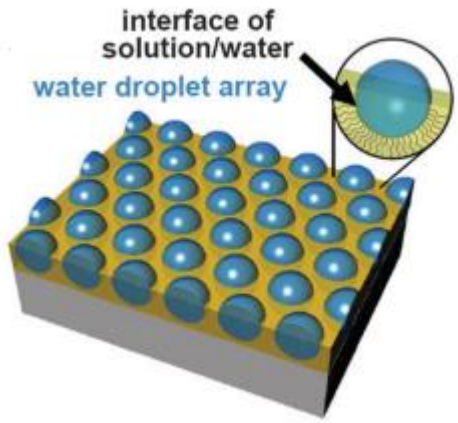

Figure 7 The example illustrates the distribution of surfactant molecules in the water-organic solvent interface during the production of honeycomb films by the BF method [91].

7. APPLICATIONS OF HONEYCOMB FILMS

Tissue engineering can be done by using the porous films with appropriate structure such as surface properties, pore sizes, thickness, and distance between pores [92]. Honeycomb films have shown to enable cell adhesion and proliferation, and to modulate cell behavior such as growth, apoptosis and differentiation. Polymer films with honeycomb structure can deliver cells to the correct site, improve cell survival, enhance cell integration and direct cell differentiation, providing a promising platform for cell transplantation. On the other hand, the different conditions such as polymer, solvent and surfactant produce films with different properties, which can be applied in different types of cell cultures as shown in Table 3.

Table 3 Various studies where honeycomb films have been used in tissue engineering applications

Polymer	Solvent	Surfactant	Pore size	Cells	References
PCL	Chloroform	CAP*	5 µm	Porcine aortic endothelial cells	[93]
PCL	Chloroform	CAP*	3 µm	Cerebral cortices of embryonic 14 days mice	[94]
PCL	THF		3.5 µm	Mouse preosteoblastic MC3T3-E1 cells	[95]
PLA	Chloroform, THF, Ethyl acetate		2.95-3.55 µm	MG-63 osteoblast-like cell lines	[96]
PLA	Chloroform	DOPE	248+ - 65 nm	Adipose-derived stem cells (ASCs)	[97]
PLA	Chloroform	DOPE	3 µm	NIH3T3 fibroblast cells	[98]
CAP	Chloroform		5 µm	Hepatocyte	[99]
PLGA	Chloroform, THF, Ethyl acetate		3-4 µm	MG63 Osteosarcorma cell line	[100]
Copolymer of dodecylacrylamide and ω-carboxyhexylacrylamide	Benzene		2.1 µm	Mimicking cells of lipid molecules and proteins	[101]

8. CHARACTERIZATION OF HONEYCOMB FILMS

The honeycomb films can be characterized in term of structure and physical properties. From the structural point of view, the observations can be done in various ways such as optical microscopy, atomic force microscopy (AFM) and scanning electron microscopy (SEM) to investigate the morphology of the films [102].

8.1 Atomic Force Microscope (AFM)

Atomic Force Microscopy (AFM) is used to create the 3D images with high resolution, and it can provide 1000 times better resolution than a standard microscope [103]. The AFM is mainly composed of two parts. The first one is the scanner modules, which can move the direction of X, Y and Z plain. The second part is the detection system according the Hooke's law, which includes a laser source, a cantilever, a mirror, a photodiode, a photo detector, and computer control [104] (Figure 8). The images are obtained from the surface of samples via AFM due to the laser guidance which is focused onto the back of the reflective cantilever. The scanner module can be seen as a tip, which scans the surface of the sample and the laser beam from the tip is reflexed from the cantilever into the photodiode. After that, the upper and lower photodiodes show the difference of light intensity, which is then sent to a photo detector. The photo detector then sends the signal to the computer control feedback loop, which is manipulated so that the distance between cantilever and sample remain constant [105]. The images are transferred to the software and can be manipulated accordingly so as to measure pore sizes, pore distribution in a certain region and overall 3D images.

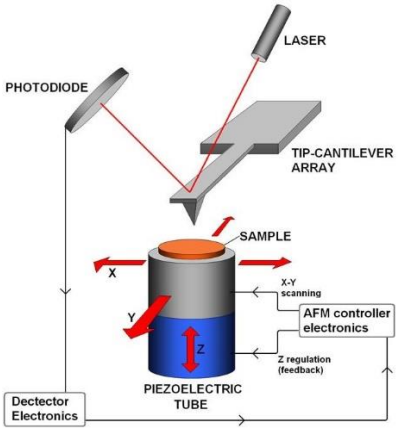

Figure 8 The simple mechanism of AFM [106]

8.2 Contact angle measurement

Contact angle is the common way to measure the wettability of the surface of the material. Wetting can be seen as the way a liquid deposed on a solid substrate spreads out or forms a certain boundary on the surface. This behavior of a liquid on the substrate can be measured by the contact angle, which the liquid forms in contact with the solids or liquids. The smaller contact angle means the larger wetting area measured boundary to boundary of the liquid or lower surface tension. A wetting liquid is a liquid that forms a contact angle with the solid which is smaller than 90º. A non-wetting liquid creates a contact angle between 90º and 180º with the solid [107].

In material science, the contact angle is used to measure the angle that a liquid creates with a solid surface or capillary walls of a porous material when the liquid and the material come in contact together. The angle refers to the interaction between solid and liquid, which is ascribed to cohesion and adhesion forces (intermolecular forces). The cohesive such as hydrogen bonds and Van der Waals stabilize similar molecules like between the liquid molecules. In contrast, the adhesive forces between dissimilar molecules such as between the liquid and solid molecules will determine the contact angle created in the solid and liquid interface [108].

From Figure 9:

- Smaller contact angle - cohesive forces are weaker than adhesive forces and molecules of the liquid tend to interact more with solid molecules than with molecules of liquid.
- Larger contact angle - cohesive forces are stronger than adhesive forces and the molecules of the liquid tend to interact more with each other than with the molecules of the solid substrate.

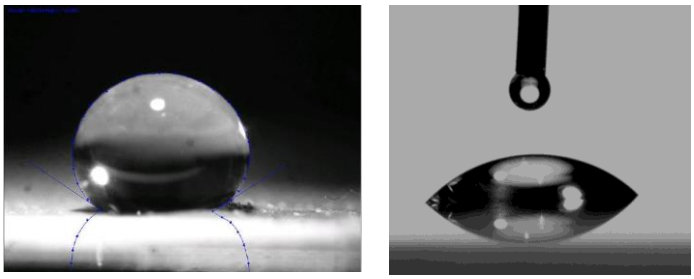

Figure 9 Hydrophobic surface showing a high water contact angle (left) and hydrophilic surface showing a low water contact angle (right) [109]

EXPERIMENTAL PART

9. METHODOLOGIES

9.1 Materials and chemicals

All chemicals and solvents were prepared according to the experiment as mentioned in the methods. Poly-L/D-lactide 50/50 (PLDLA), Polycaprolactone (PCL), Ethyl acetate (97%), Tetrahydrofuran (THF), TWEEN® 80 and Polyvinyl alcohol (PVA) were purchased from Sigma-Aldrich Company. The humidity level in the environment or percentage of relative humidity (RH %) was also controlled according to the experiment using the humidity chamber (water, mobile fan in the chamber and hygrometers) at room temperature (25 ºC). Small glass containers or vials were used to store various polymer solutions in different concentrations. Glass Petri dishes with 30 mm diameter were also used for making the thin films.

9.2 Instruments

The equipment and instruments used during the thin film preparation included a digital scale (METLER TOLEDO, AB265-S/FACT), a magnetic stirrer with heating system (IKAMAG RCT), an optical microscope (Olympus, BH-2, GWB), Atomic force microscope (AFM, XEI, XE-100, XEC-AVT Marlin F080C, Park Systems Corp), micro meter (Mitutoyo) and water contact angle was measured by the sessile drop method at room temperature using a Theta Lite optical densitometer (Attension, Biolin Scientific AB, Sweden).

9.3 Methods

This research work followed the experimental sequence as shown in Figure 10. In the beginning, various types of polymer films were prepared by changing parameters such as polymer concentration, solvent, humidity and surfactant. After that, the films were investigated in term of the structure, pore sizes, pore arrangement, thickness and contact angle. Lastly, the most promising polymer films were tested in cell culture.

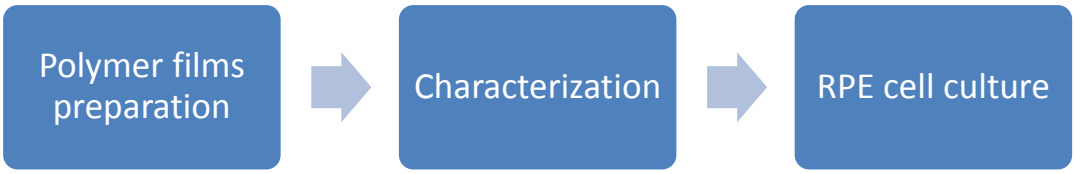

Figure 10 The simplified flow chart of the experiments which included polymer films preparation, characterization and RPE cell culture.

9.3.1 Preparation of polymer films

Polymers have been prepared in different concentrations to observe the effect of polymer concentration on the formation of porous films. For instance, PLA (polylactide) gilms with 50/50 L/D ratio were prepared at 50, 45, 40, 26, 20 and 10 mg/ml. Polycaprolactone (PCL) was also applied for the experiment. TWEEN®80 was used as surfactant and prepared around 30 mg per each experiment, then diluted with 1 ml of ethyl acetate to different concentrations: 1, 0.5, 0.2, 0.1, 0.05 and 0.01 % (w/v).

The effect of different processing parameters on the film properties was investigated, namely type of polymer, polymer concentration, type of surfactant, surfactant concentration and humidity level in the environment. The observed film properties were porosity, size of pores, homogeneity of the thin film, pore distribution, pore structure, pore distribution and the thickness of the films. The porous films were produced in the humid chamber after casting the polymer solution with or without surfactant in the Petri dish. In the humid chamber, there was a moisture sensor, a temperature meter and also a mobile fan. High velocity of wind flow from the mobile fan was used to achieve fast deposition of water droplets and fast solvent drying, thereby forming the honeycomb film.

- *Polylactide (PLDLA)*

Various PLA films were fabricated using ethyl acetate as solvent and some of the PLA solutions prepared with surfactant such as TWEEN® 80 and PVA as well as without surfactant. To explain briefly, the polymer granules were weighted and dissolved in the correct volume of solvent, which was ethyl acetate or THF. The concentration of PLA on the experiment was 10, 20, 26 and 40 mg/ml as seen in Figure 11.

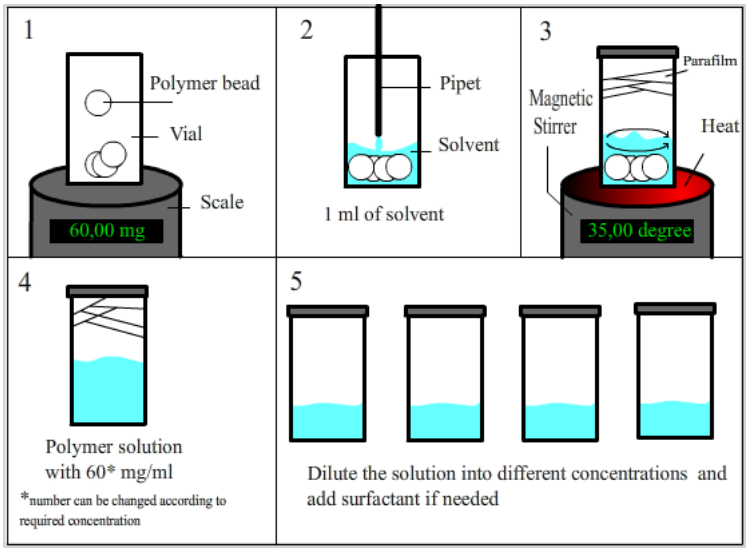

Figure 11 Simplified process of preparing polymer solutions

Each solution was allowed to dissolve at 45-50ºC until homogeneous. As observed in Figure 12, 500µl of each solution was cast into a 30 mm diameter the Petri dish making sure that the solution covered the bottom at the dish entirely. The petri dishes were then transferred to the chamber in order to dry the sample in the proper humidity level normally between 85 and 90% of relative humidity (RH %).

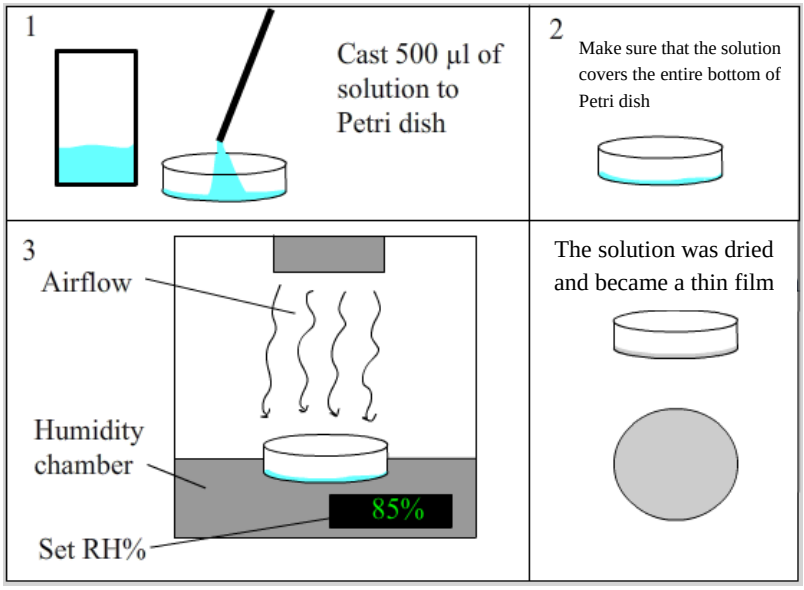

Figure 12 The diagram shows how the thin film is prepared

After the samples were dried, they were removed from the chamber, and then washed with 70% ethanol in order to remove the surfactant. The samples were cleaned by ethanol 3 times using around 1000 µl each time. After that, the samples were dried at room temperature for several hours and put in the vacuum chamber in order to remove the residual water content, until further analysis. The investigation of the structure was

done by visual inspection or by microscopy (optical microscopy and AFM). Moreover, water contact angle was also used to investigate the hydrophobic and hydrophilic properties of the polymer films. Humidity level in the chamber (RH%) was also taken into account that it might result as the size of pores, homogeneity of the polymer surface, pore distribution, and the film thickness which the RH% was adjust to current level, 65, 75, 85 and 95 % accordingly.

- *Polycaprolactone (PCL)*

For polycaprolactone (PCL), the procedure was the same as PLDLA except that the dissolving time was increased to more than four hours in order to ensure complete dissolution. After casting, the solution was then dried in the chamber for 30 minutes to 1 hour. The samples were removed from the chamber, and then washed gently with 70% of ethanol. The characterization of the films was also done in the same way as for PLA.

- *Surfactant*

Two different surfactants were investigated to produce the honeycomb films, namely TWEEN® 80 and polyvinyl alcohol (PVA). TWEEN® 80 was prepared at the concentration: 1, 0.5, 0.2, 0.1, 0.05 and 0.01 % in the polymer solution.

For PVA, the concentration was 5, 2, 1, 0.5, and 0.1%. The solution was prepared as described previously, but the PVA cannot dissolve well in ethyl acetate. In this case, the PVA beads were dissolved in distilled water until the solution became homogeneous. After that, 3 ml of distilled water was cast in the bottom of Petri dish before casting the polymer solution and surfactant in order to form the breath figure array in the humidity chamber as seen in Figure 13. The experiment was performed similarly to the sample without surfactant.

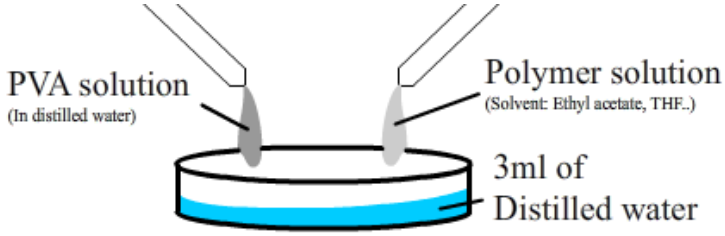

Figure 13 The preparation of polymer films using PVA as surfactant

9.3.2 Characterization of polymer films

The observation of film properties was done via optical microscope, AFM and also the physical characterization performed via measuring the water contact angle to investigate the hydrophilic and hydrophobic properties of the surface (Figure 14). Both the top and bottom surfaces of films were observed. Moreover, the thickness of the films was also studied. The experiments were repeated at least 3 times to get reliable results. The investigated properties of the films were pore sizes, pore distribution, homogeneity of the film, thickness, water contact angle, permeability and cell behavior when cultured on the films.

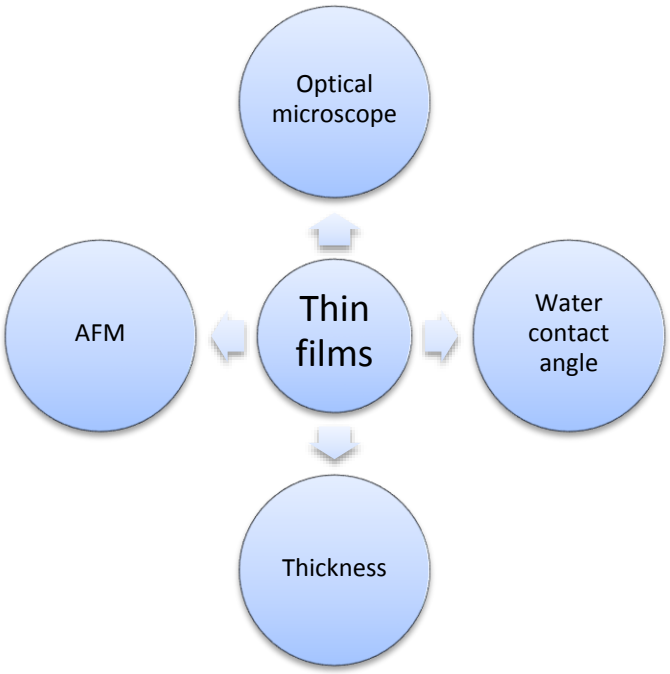

Figure 14 The flow chart representing the characterization of honeycomb films.

- *Structural characteristics*

The homogeneity was seen from the surface by visual observation. A homogeneous film was considered to have even distribution of the polymer, covering all area. The optical microscope was the first step of characterization and it was used to briefly observe the surface and pore sizes. In addition, an attached camera on the microscope was used to capture the image of the films, which were transferred to the software with image processing in order to measure the pore sizes and the pattern of pores. In cases where samples could not be analyzed by optical microscopy due to high thickness and opacity, a light source placed above the sample was used. The 20x of magnification was chosen observe the polymer films, which was found suitable to observe pore sizes. The pores in the images were measured and chosen randomly around 20-40 units to get most reliable results. Results were used to calculate the average and standard deviation (SD).

In AFM samples, the process of measurement was done according to the instructions such as adjusting scan rate (0.5 Hz) and scanning area (30 μm^2). An APPNANO AFM cantilever was used as probe with type ACTA, 125 μm of length, tip radius < 10 nm, f = 200−400 kHz, spring constant = 25−75 N m−1, coating aluminum. The homogeneous area of each sample was chosen to scan in non-contact mode. The analysis was done under air at room temperature. At last, the images were analyzed via AFM software (XEI image processing, Park Systems) in order to measure pore size and to observe more details of the surface.

- *Water contact angle measurement*

The common way to measure the wettability of material surface is to use the water contact angle method. In the experiment, a water droplet was applied to the surface of porous films. The camera detected the image and measured the left and right angle the water drop. The samples were cut in the middle area and measured 3 times in different regions of each piece.

- *Films thickness*

The thickness of thin films can vary when different conditions are used, such as polymer concentration, type of solvent, solubility, percentage of relative humidity (RH%) and the ambient environment. In this work, thickness was measured by micro meter. The samples were removed from the Petri dish with tweezers and then the thickness was meaured in the middle part of the film around 3 times to ensure the reliability.

9.3.3 Retinal pigment epithelium cell culture (RPE cell culture)

After the preparation and characterization of honeycomb films, the most promising films (presenting honeycomb patterns) were tested in the cell culture laboratory as substrate materials for RPE cells. The experiment was carried out by my supervisor in order to see the cell behavior on polymer films.

This stage began with using hESC line Regea 08/017, which was differentiated to RPE cells according to the methods employed by the research unit [110]. Before plating the cells, samples were treated with 70% ethanol for 20 minutes for disinfection and washed twice with sterile Dulbecco's Phosphate Buffered Saline (DPBS). Then, polymer films were coated with human collagen IV (5µg/cm^2) for 3 hours at 37 °C. After that, the films were rinsed twice with DPBS to remove any unbound protein and undesired substances. RPE cells were suspended into DM- medium and were cultured on the membranes at a density of 180,000 cells/cm^2 for 9 days.

9.3.4 Phalloidin and DAPI Staining

First of all, cells were rinsed with DPBS two times and then fixed with 4% paraformaldehyde (Sigma-Aldrich) for 10 minutes at room temperature. Cells were washed three times with DPBS three times and permeabilized of the cells with 0.1% Triton X-100 in DPBS (Sigma-Aldrich) at room temperature for 10 minutes. After that, cells were washed three times with DPBS and were stained with phalloidin in 3% BSA-PBS for 20-30 minutes at room temperature followed by rinsing three times with DPBS for 5 minutes. Films were placed on a cover slip and were briefly dried. Vactashield mount with DAPI was added immediately and another cover slip was added to seal the films. Samples were visualized in the fluorescence microscope for the localization of actin filaments and nuclei.

10. RESULTS AND DISCUSSION

PCL and PLA were investigated as film-forming materials. Film properties such as pore sizes, honeycomb pattern and pore distribution were analyzed. In this section, results of the characterization of polymer films are presented after analysis of films by optical microscopy, atomic force microscopy, water contact angle measurements and thickness determination. The different methods provided different information, for example, the pore sizes were acquired from optical microscopy and AFM. To analyze in detail, the AFM was applied because of the lower resolution of the optical microscope and difficult visualization of opaque films by this technique. Moreover, the AFM software (XEI) allowed the accurate determination of pore sizes and pore distribution. All the results are illustrated below accordingly. In addition, films were analyzed in terms of homogeneity of polymer distribution.

10.1 Film thickness

Ideally, thickness should be around 2-4 μm, so it would similar to the Bruch's membrane, where the RPE cells locate in the retina. However, thin films can be very difficult to surgically implant, and thicker materials (< 50 μm) can be considered suitable for this purpose. In the absence of surfactant, increasing concentration of PLA in ethyl acetate from 10 to 40 mg/ml caused thicker polymer films as a result: 6 to 15 μm (Table 4). For PCL, a similar trend was found, but the films were even thicker; 14 to 19 μm. Complete solvent evaporation of PLA and PCL occurred up within 30 minutes under 85% of humidity; the typical thickness on average of polymer films was around 15 μm. In contrast, polymer with surfactant shows different results, in which the surfactant tends to change the characteristics of the polymer solution into more hydrophilic. As a result, the polymer dissolves better than without surfactant and the polymer solution could spread easier. However, the surfactant concentration did not seem to affect the results clearly, particularly when surfactant concentration was increased. However, excessive concentration of surfactant affects the film structure that it can no longer maintain its shape and the films become destroyed. Solvent was also taken into account because the choice of solvent can affect dissolvability of the polymer, which can make the film thicker or thinner.

In our work, the results did not show an obvious difference in the thickness of films when the polymers were dissolved in ethyl acetate or THF films.

Table 4 Thickness of films prepared in this work

Polymer	Polymer concentration	Solvent	Surfactant	Surfactant concentration	Thickness (μm)
PLA	10 mg/ml	Ethyl acetate	-		6
PLA	20 mg/ml	Ethyl acetate	-		7
PLA	26 mg/ml	Ethyl acetate	-		12
PLA	40 mg/ml	Ethyl acetate	-		15
PLA	26 mg/ml	Ethyl acetate	Tween 80	0.1%	8
PLA	26 mg/ml	Ethyl acetate	Tween 80	0.5%	13
PLA	26 mg/ml	Ethyl acetate	Tween 80	1%	Torn into pieces
PLA	26 mg/ml	Ethyl acetate	PVA	0.5%	60
PLA	26 mg/ml	Ethyl acetate	PVA	1%	60
PLA	26 mg/ml	Ethyl acetate	PVA	2%	60
PLA	26 mg/ml	Ethyl acetate	PVA	5%	60
PLA	26 mg/ml	THF	-	-	11
PLA	26 mg/ml	THF	Tween 80	0.1%	8
PCL	10 mg/ml	Ethyl acetate	-		14
PCL	20 mg/ml	Ethyl acetate	-		16
PCL	30 mg/ml	Ethyl acetate	-		17
PCL	40 mg/ml	Ethyl acetate	-		19
PCL	40 mg/ml	Ethyl acetate	Tween 80	0.1%	18
PCL	40 mg/ml	Ethyl acetate	Tween 80	0.5%	21
PCL	40 mg/ml	Ethyl acetate	Tween 80	1%	38
PCL	30 mg/ml	THF	-		17
PCL	30 mg/ml	THF	Tween 80	0.1%	9

10.2 Film homogeneity and porosity

The results show the comparison of films prepared using different polymer types, polymer concentration, solvent, surfactant and percentage of relative humidity (RH %). The optical microscope was used to analyze the general microstructures of the films such as pores and honeycomb pattern on the polymer surface. AFM was used to create the 3D images from the samples, allowing the observation of the surface and roughness properties. AFM is however time-consuming and unpredicted factors such as noise, interference from other electric sources and other undesired signals can disrupt the image data. So, the samples were chosen carefully for AFM analysis. The most promising films (as observed by optical microscopy) that were analyzed by AFM: PLA in ethyl acetate with various surfactant types and concentrations (0.05-0.2% of Tween 80 and 0.5-5% of PVA) and PCL in THF.

26 mg/ml of PLA films prepared in ethyl acetate in the absence of surfactant, and using Tween 80 and PVA as surfactants were analyzed. Each surfactant was considered in different concentrations such as 0.2% of Tween or 5% of PVA under 85% of humidity. For PCL, the successful honeycomb pattern was produced by mixing the polymer solution with THF under 58% of moisture environment. The result will be discussed in more detail in the following sections.

10.2.1 Effect of polymer concentration

According to the images from optical microscopy (Figure 15), it can be seen that the pore sizes and distance between pores were relatively smaller and the pores became more organized with the increase of polymer content from Figure 15a to Figure 15d for PLA and Figure 15e to Figure 15h for PCL.

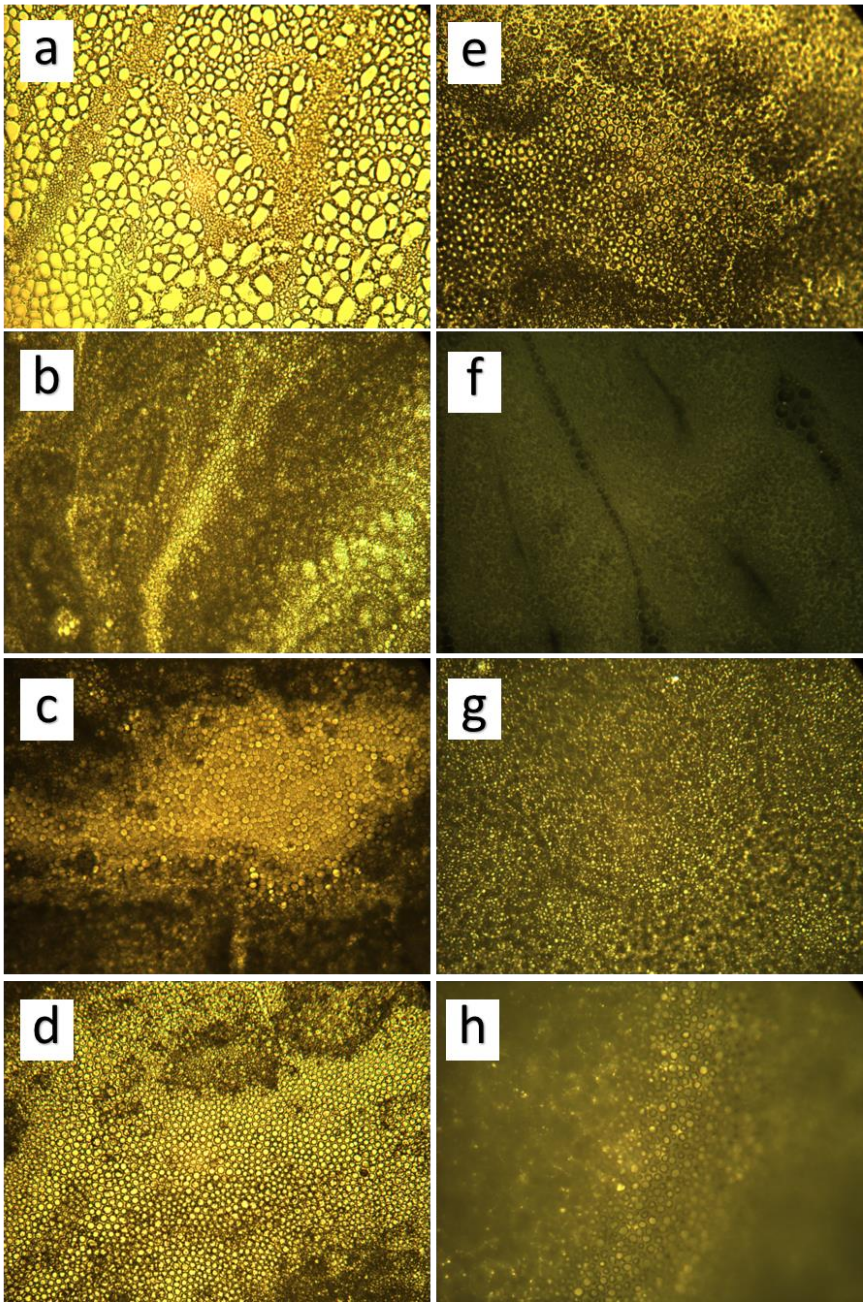

Figure 15 Images from optical microscopy at 20x magnification a) 40 mg/ml of PLA b) 26 mg/ml of PLA c) 20 mg/ml of PLA d) 10 mg/ml of PLA e) 40 mg/ml of PCL f) 26 mg/ml of PCL g) 20 mg/ml of PCL h) 10 mg/ml of PCL

The different conditions produced different films, with a wide range of pore diameter in both PLA and PCL. For PCL, Pores were presented between 4 to 8 µm of diameter as seen in Figure 16.

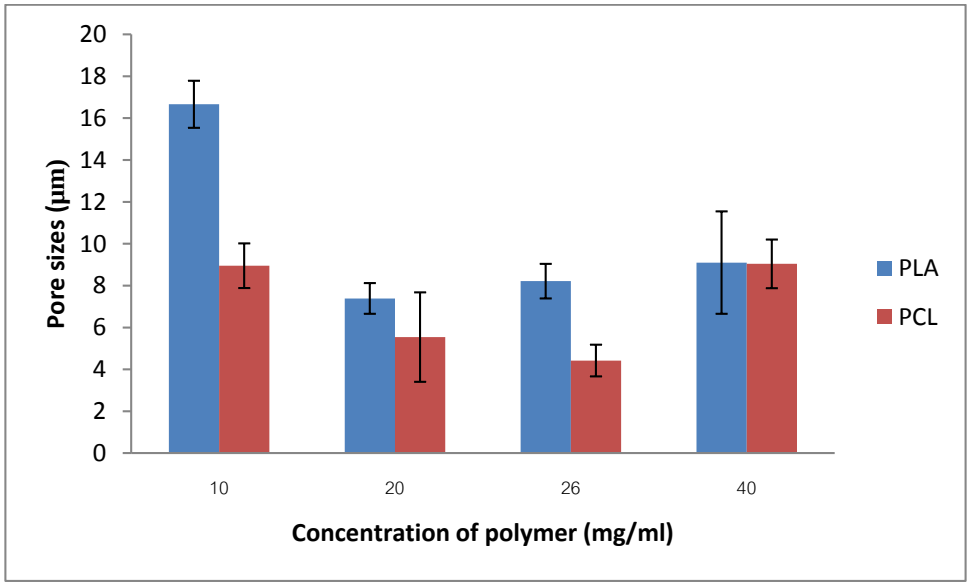

Figure 16 The graph shows the comparison of pore sizes between PLA and PCL without surfactant.

In the absence of surfactant, smaller pores were obtained when PLA and PCL concentration was increased in the sequence 10, 20, 26 and 40 mg/ml under 85-90% of humidity. For instance, 10 mg/ml of PCL formed films with pore diameter around 16 µm, while 26 and 40 mg/ml of PLA formed films with pores of only 7 and 9 µm respectively in diameter. The increase in polymer concentration from 26 to 40 mg/ml, provided smaller pores, for instance, the pore sizes PCL varied from 16 to 4 µm with increasing concentration, as observed by light microscopy and AFM.

The results show that increasing polymer concentration can increase the viscosity of polymer solution, which can decrease pore sizes because of the higher capacity of the polymer to stabilize a larger surface area of the water droplets [111].

Pore sizes should be at least 3 µm in order to produce materials that are permeable enough in order to ensure cell survival after transplantation [112]. Bigger pores are also undesirable since the cells can migrate through the membrane.

In this case, the 26 mg/ml of PLA and PCL were chosen to the next experiment by using surfactant in order to improve the quality of films because they provided the most promising results, which was smallest pore sizes and organized order of porous structure compared to higher or lower concentration.

However, the polymer did not dissolve well in ethyl acetate, which caused the films to become non-homogeneous. Only the middle part of the films was homogeneous, white and transparent, but this region was small when the concentration increased and the honeycomb array was found only in the middle of the sample as seen in Figure 17.

Figure 17 26 mg/ml of PLA and PCL films from left to right

The acquired images from AFM covered around 30 μm^2 of surface area on each sample. Films prepared using 26 mg/ml PLA in the absence of surfactant were shown to have a porous surface with heterogeneous size distribution in the range 2-7 µm. Pores did not form a honeycomb pattern as shown in Figure 18.

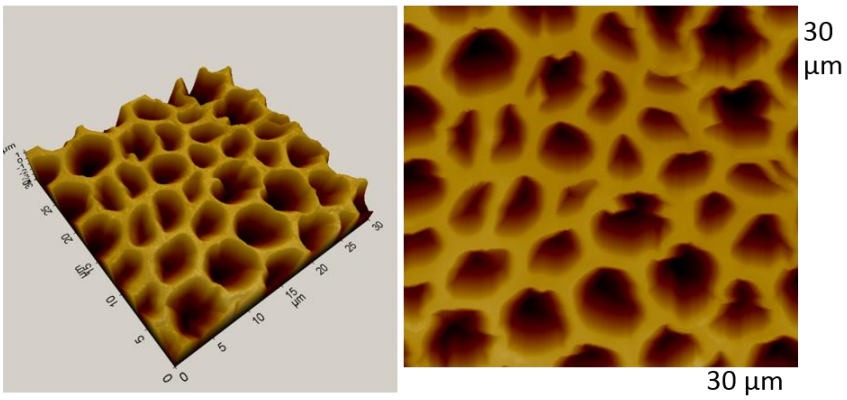

Figure 18 AFM images of a polymer films prepared with 26mg/ml of concentration, no surfactant included

10.2.2 Effect of surfactant concentration

According to the previous experiment, the results show that 26 and 40 mg/ml of PLA provided the most promising results, in terms of pore size and homogeneity of polymer distribution. Similar films were subsequently prepared by adding surfactant (Tween 80) at different concentrations, namely from 0.01 to 0.02% w/w. The results showed that higher concentration of Tween 80 formed smaller pores on the polymer films.

10.2.2.1 Tween 80

For PLA films adding 0.1% Tween 80 (dissolved with ethyl acetate), to the polymer solution resulted in a dramatic decrease of pore size and in a more ordered honeycomb pattern. Films also became more homogeneous. This is probably due to hydrophobicity of polymer solution, when using Tween 80 as surfactant, which strongly enhances droplet nucleation because the surfactant acts as wetting agent to lower surface tension between two liquids or a liquid and a solid [113]. As a result, smaller pore sizes were obtained as surfactant concentration increased. As mentioned previously, ethyl acetate is not a good solvent for PLA and could not form homogeneous films, with only a small portion of the film (on the edge of the sample, Figure 19) being homogeneous. The missing region on the film shown in Figure 19 was used as a sample for AFM.

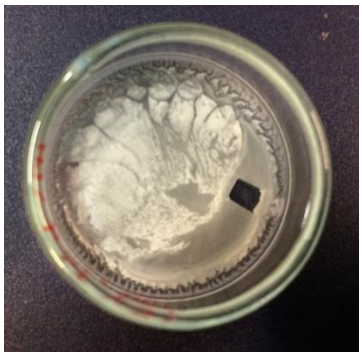

Figure 19 26 mg/ml of PLA in the presence of 0.1% Tween 80

From Figure 20 and Figure 21, it can be seen that the average pore size of the films decreased with increasing concentration of surfactant, which was 2 to 6 µm for 26 mg/ml of PLA under 85 % of humidity. However, with excessive concentration of surfactant, which is around 0.20 % or higher pore diameter increased and the films became fragile and broke easily.

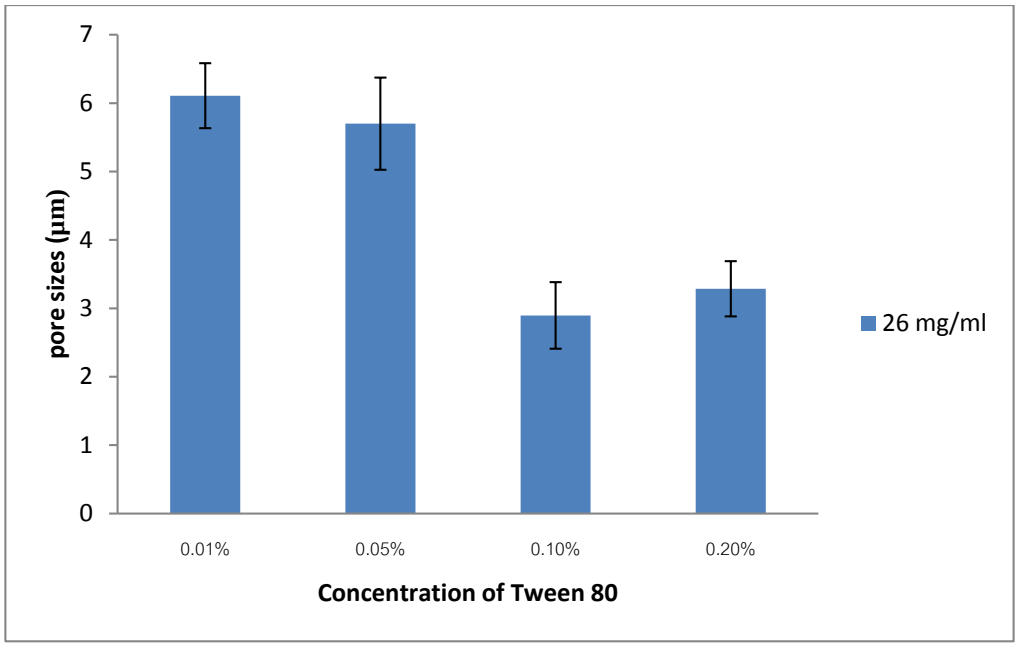

Figure 20 26 mg/ml of PLA with different concentration of surfactant that provided the various pore sizes.

It was additionally shown that increasing PLA concentration in the presence of 0.1% of Tween 80 increased pore sizes as well, namely from 3.8 µm to around 8-9 µm as shown in Figure 21. The range between 26-30 mg/ml provided the best results in terms of the formation of a homogeneous honeycomb pattern, homogenous polymer distribution and small pore sizes (Figure 21).

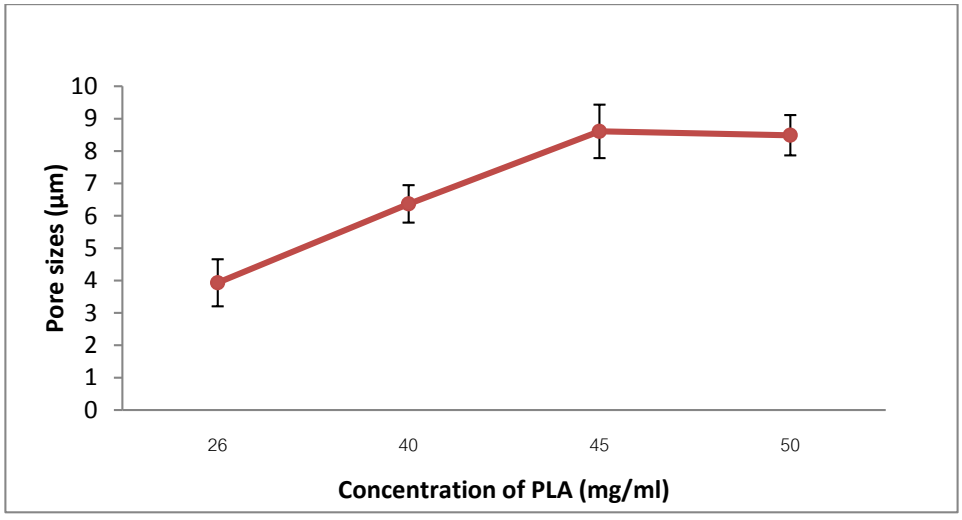

Figure 21 The trend of pore size when increasing amount of PLA in the presence of 0.1% Tween 80

Moreover, the images from optical microscopy from Figure 22a to Figure 22d show that increasing surfactant concentration resulted in smaller pores and higher organization of pores.

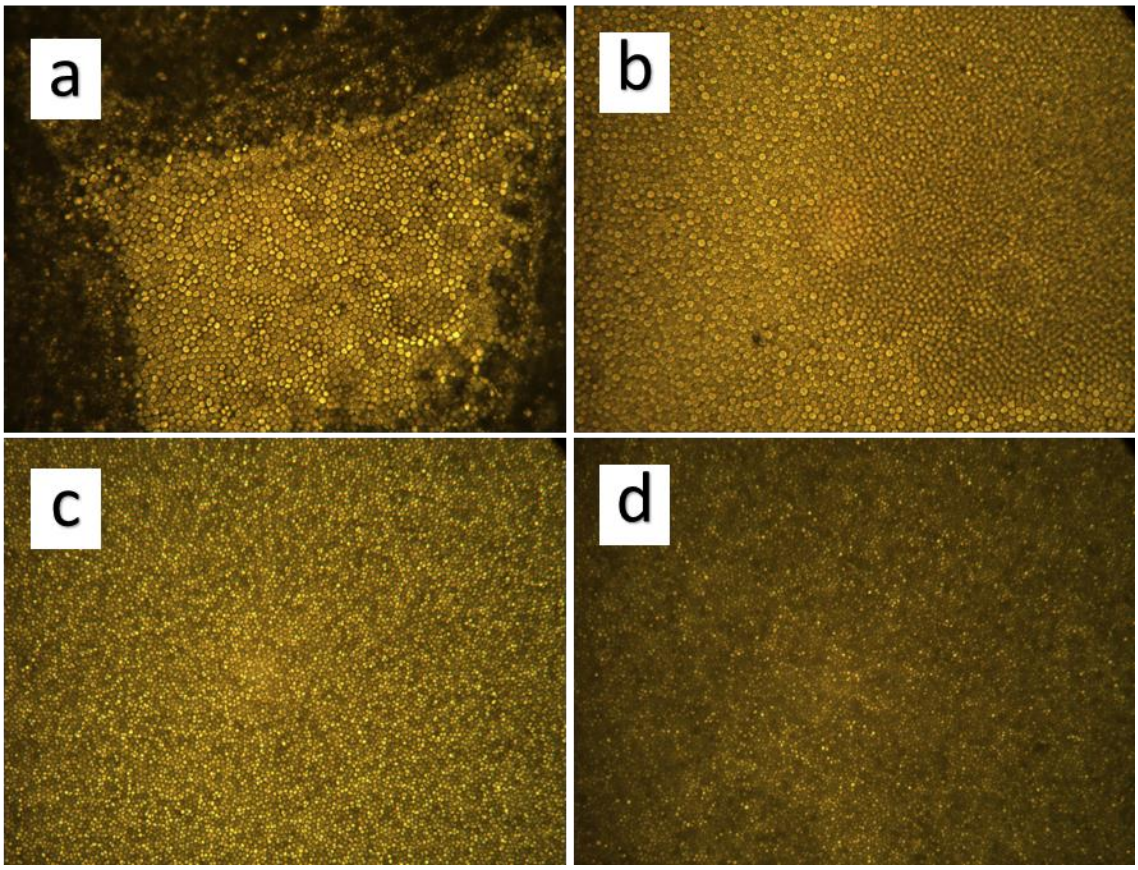

Figure 22 Optical microscopy (20x magnification) images of polymer films prepared using: a) 26 mg/ml of PLA with 0.01% of Tween 80 b) 26 mg/ml of PLA with 0.05% of Tween 80 c) 26 mg/ml of PLA with 0.1% of Tween 80 d) 26 mg/ml of PLA with 0.2% of Tween 80

- *26 mg/ml of PLA with 0.05% Tween 80*

Figure 23 shows the pattern of honeycomb where the pores can maintain their round shape nicely with a relatively uniform size distribution. This means that the surfactant could help the polymer solution to maintain the water droplets and create the porous structure on the surface. PLA solution in ethyl acetate with Tween 80 prepared with 26 mg/ml of polymer concentration and 0.05% of surfactant, under 85% of humidity showed a good honeycomb array due to the nucleation on the surface, which increased in the same rate as increasing in concentration of surfactant and amphiphilicity of polymer solution, in which water vapor condenses rapidly on the surface. Moreover, the surfactant also helps to maintain high interfacial tension as well as to preserve the pore structure steadily and ensure that the hydrophilic regions are fully wet. A high concentration of hydrophilic groups causes the droplets to interact very early during the process, so coalescence occurs.

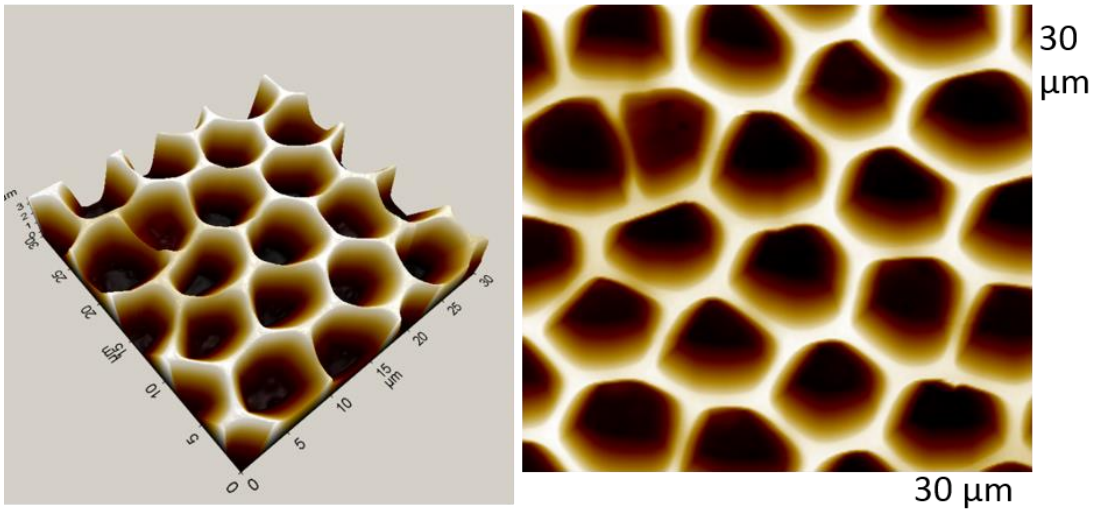

Figure 23. AFM images of film prepared using 26mg/ml of PLA with 0.05% of Tween 80

- *26 mg/ml of PLA with 0.1% Tween 80*

From the previous successful honeycomb film, polymer films were prepared in the presence of 0.1 % Tween 80 and also observed by AFM to investigate the porous structure. The results provided even better surface features than 0.05% Tween 80 with highly ordered pores and perfect honeycomb-like distribution. Moreover, the pore sizes were approximately of the same size, around 2 to 3µm as shown before by optical microscopy (Figure 20) and as confirmed by AFM (Figure 24).

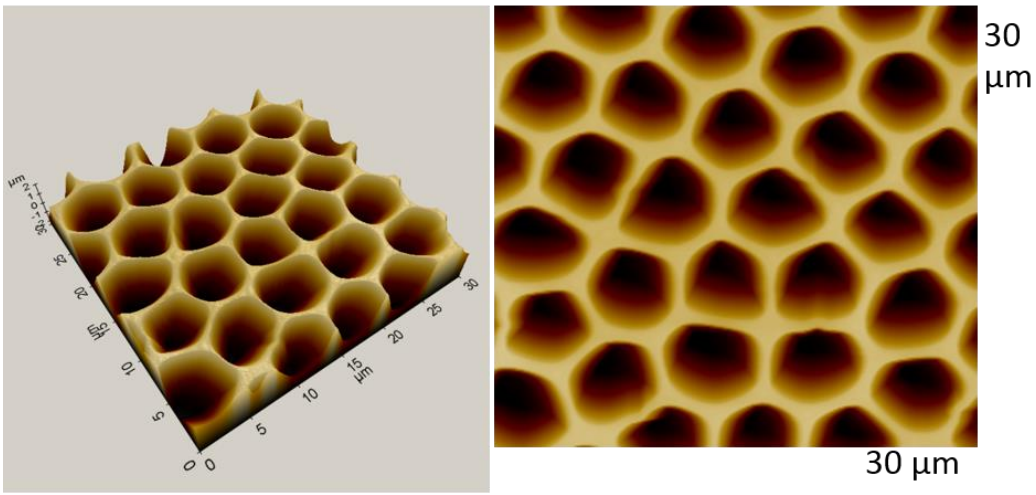

Figure 24. AFM images of film prepared using 26mg/ml of PLA with 0.1% of Tween 80

- *26 mg/ml of PLA with Tween 80 0.2%*

Polymer films produced in the presence of 0.2% Tween 80 showed that the pores cannot maintain their shape under the humid environment because excessive surfactant can reduce surface tension and make the polymer surface more fragile (Figure 25).

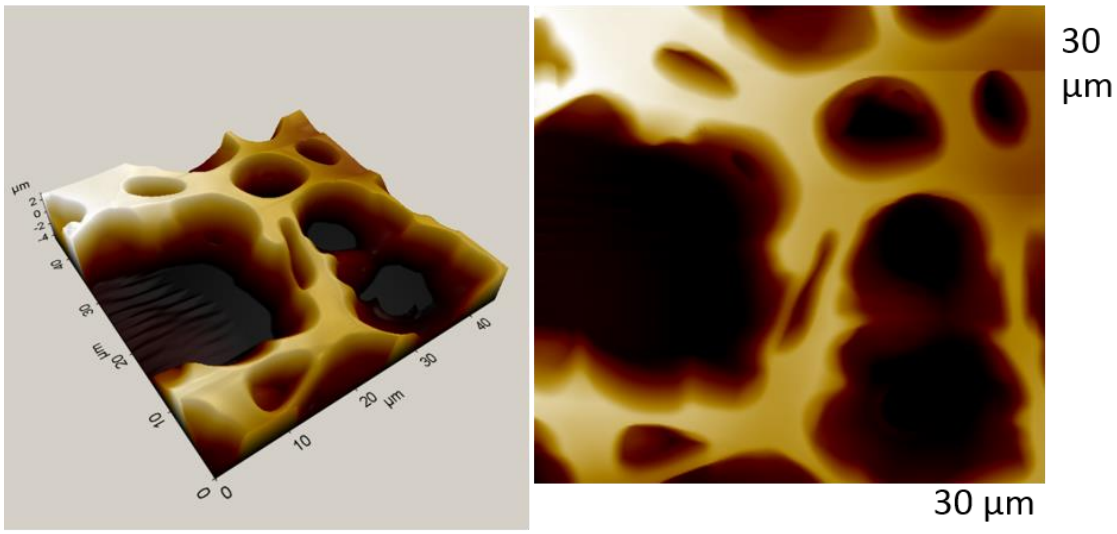

Figure 25 AFM images of film prepared using 26mg/ml of PLA with 0.2% of Tween 80

- *30 mg/ml of PCL with Tween 80*

Optical microscopy analysis showed that 26 mg/ml of PLA and 30 mg/ml of PCL provided the most promising results, i.e. pore sizes were around 2-3 µm and formed honeycomb films. In subsequent experiments, the concentration of surfactant. Tween 80 was varied between 0.01 to 0.20% in order to establish the influence of surfactant concentration on PCL film properties.

The results from Figure 26 showed that increasing concentration of Tween 80 in PCL caused an increase in the pore diameter. However, when surfactant concentration was higher than 0.10%, the pores were not formed and the pattern on the films was inhomogeneous.

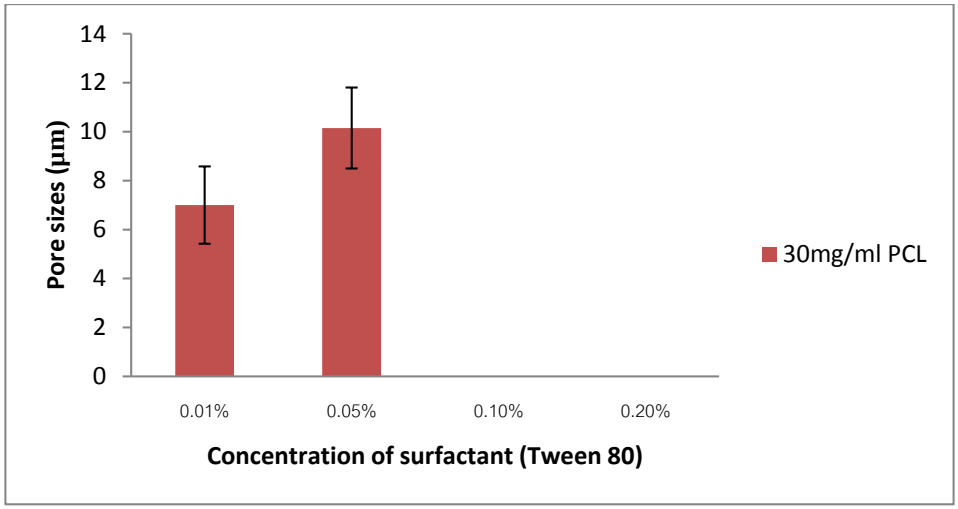

Figure 26 Effect of surfactant concentration on pore size of PCL films

10.2.2.2 Polyvinyl alcohol (PVA)

Samples were prepared using different concentrations of PVA namely 0.5, 1, 2, and 5% under 85% of humidity at room temperature. The films could maintain their shape on the distilled water and were shown to be homogeneous in the central region, as shown in Figure 27.

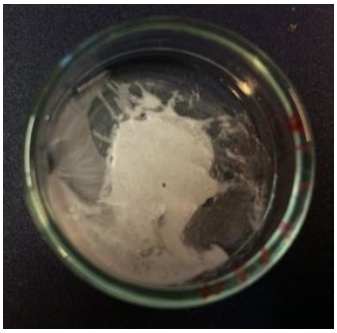

Figure 27 26 mg/ml PLA with PVA film

AFM results are shown in Figure 28. It can be seen that higher concentration of PVA leads to higher distribution of pores on the polymer film due to the same reason of amphiphilic polymer, which can enhance the nucleation rate of pores on the polymer surface. In this case, pore numbers on the film increase simultaneously with the higher concentration of surfactant. PVA lacks of capability to dissolve in ethyl acetate, in which distilled water can dissolve the PVA granules better. In addition, it has been shown that honeycomb patterns can also be produced when the polymer solution is cast on a water surface [114].

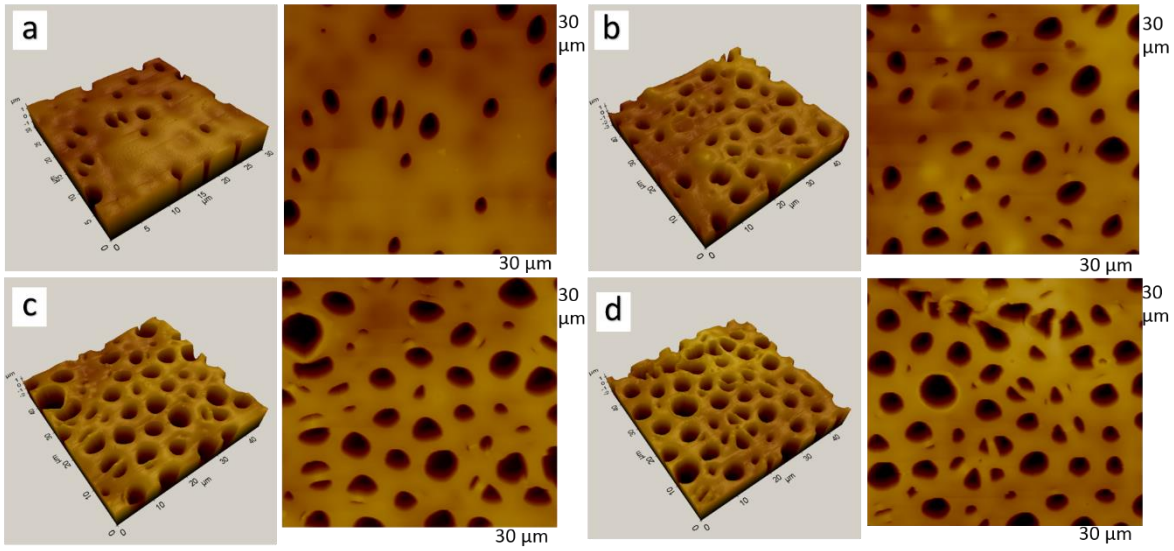

Figure 28 AFM images of honeycomb structure of polymer films: a) 0.5% b) 1% c) 2% d) 5% of PVA

From Figure 29, it can be seen that changing surfactant concentration can affect pore size and pore distribution in some areas. Pore sizes did not significantly change (Figure 29 a). However, the number of pores increased dramatically when PVA concentration was increased from 0.5 to 5% (Figure 29 b).

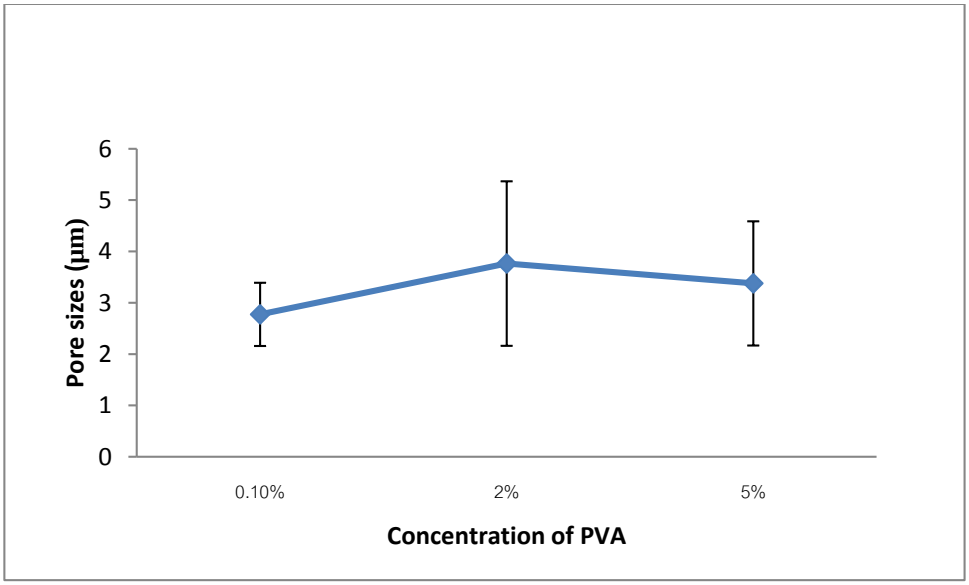

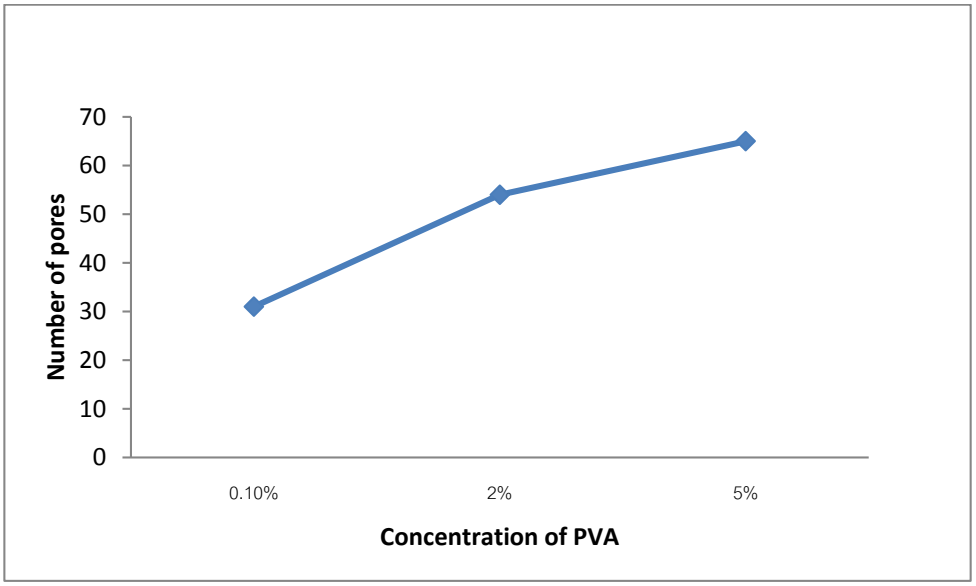

Figure 29 The graphs show the pore size (a) and number of pores (b) related to increasing concentration of surfactant, PVA in PLA

10.2.3 Effect of solvent

In this experiment, two different solvents were used and compared: ethyl acetate and THF, in order to define the effect of changing solvent on film properties. Ethyl acetate was used first place to dissolve PLA and PCL. Moreover, it was used to dilute the polymer solution to various concentration such as 10 to 40 mg/ml from 60 mg/ml. It took several hours to dissolve PLA and PCL because ethyl acetate is not the best solvent for those polymers, but it has less toxicity and higher biocompatibility compared with tetrahydrofuran (THF) and chloroform. For instance, according to the FDA standard, THF and chloroform are considered a class 2 solvent because of inherent toxicity. Ethyl acetate is in the class 3 solvent, which may be regarded as less toxic and of lower risk to human health. In addition, long-term toxicity could not be found in the studies of solvent in class 3 as seen in the Table 5 [115].

Table 5 The comparison of toxicity of the solvents used in this study according to FDA standard [115]

Solvent	Class	PDE(mg/ml)	Concentration limit (ppm)
Chloroform	2	0.6	60
Tetrahydrofuran	2	7.2	720
Ethyl acetate	3	50 or less	5000

Samples prepared with PCL in THF could dissolve better than using ethyl acetate as solvent, but THF has higher toxicity. In this case, films were much more homogeneous as compared to films prepared in ethyl acetate. Increasing polymer concentration (more than 26 mg/ml) led to even smaller pore sizes than PCL in ethyl acetate due to the higher solubility of the polymer in this solvent (Figure 30).

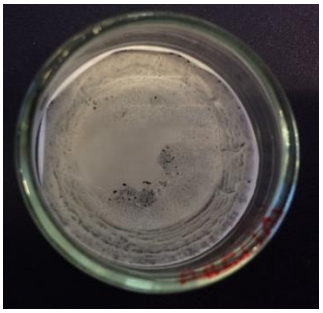

Figure 30 PCL films prepared THF as a solvent

The humidity value is important to consider in this issue because the results from PCL films clearly showed that lower RH% could form smaller pore sizes compared with higher RH% due to the high density of water droplets in the air, which caused larger pores on the polymer surface. Surfactant in PCL solution (dissolved in THF) could not help the polymer film to form the honeycomb. PCL is best to work alone dissolved in THF without any surfactant to form BF array under 55% humidity.

From Figure 31, pore sizes decreased from 9 to 4 with increasing concentration of PCL (from 10 to 40 mg/ml) when THF was used as solvent, while the opposite tendency was observed when ethyl acetate was used.

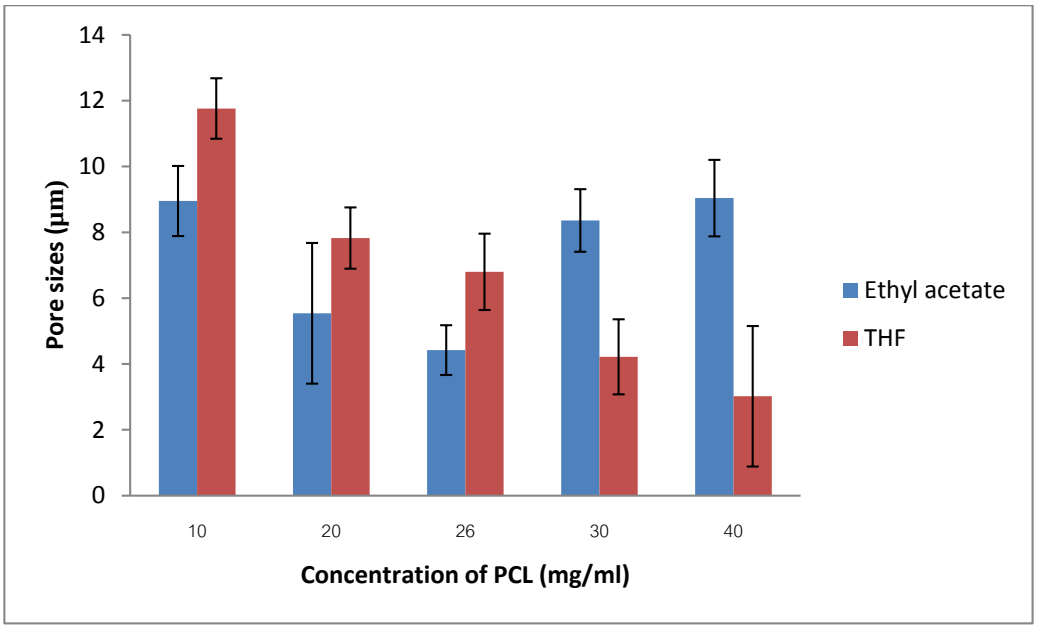

Figure 31 The comparison of PCL in ethyl acetate and THF.

For PLA films (dissolved in ethyl acetate), the polymer cannot dissolve properly with ethyl acetate which caused the formation of non-homogeneous films. From the Figure 32, it can be seen that pore sizes slightly decreased from 12 to 3 µm when the concentration increased from 10 to 40 mg/ml of PLA. However, the pores were not clearly formed when THF was used as solvent and the honeycomb pattern cannot be seen in those films.

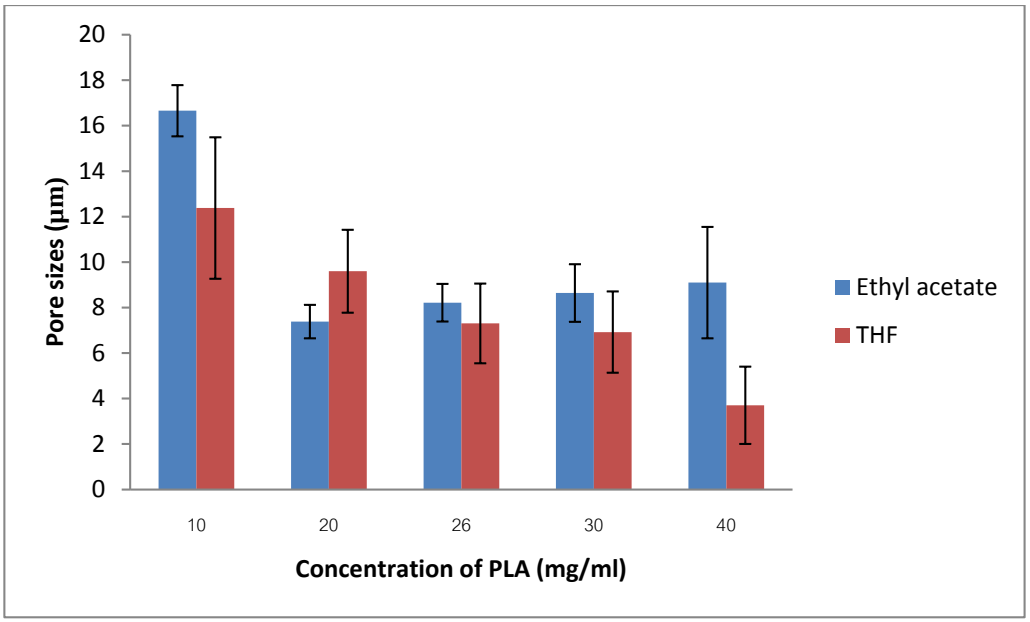

Figure 32 The comparison of PLA in ethyl acetate and THF.

Optical microscopy images (Figure 33), it shows that the alignment of pores was relatively better and pore sizes became more even with increasing concentration of PCL in (Figure33a to 33e). For PLA films (Figure 33f to 33j), the pore sizes were randomly formed on the film without forming honeycomb pattern and sizes were not even.

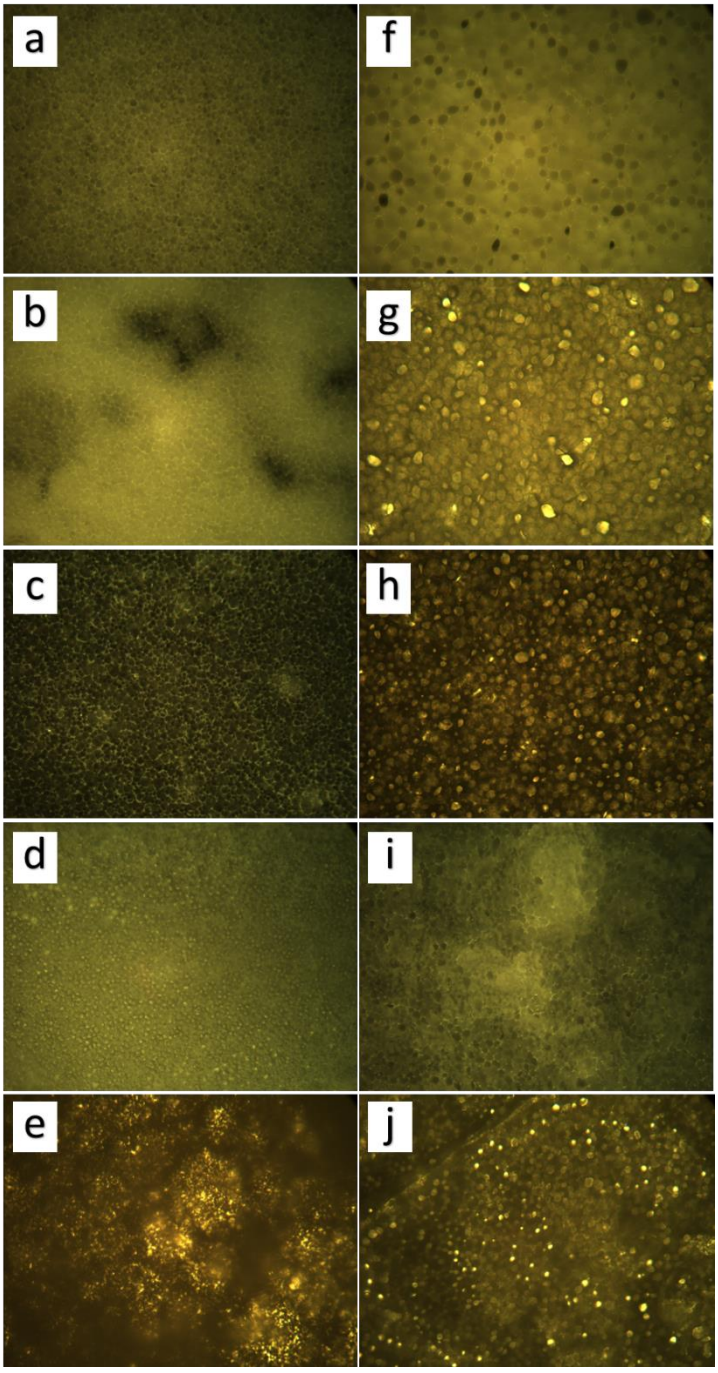

Figure 33 Optical microscopy images, 20x magnification: a) 10 mg/ml of PCL b) 20 mg/ml of PCL c) 26 mg/ml of PCL d) 30 mg/ml of PCL e) 40mg/ml of PCL f) 10 mg/ml of PLA g) 20 mg/ml of PLA h) 26mg/ml of PLA i) 30 mg/ml of PLA

From AFM image (Figure 34), PCL films in THF had higher roughness on the outer surface and the pores were randomly formed, covering the entire film, but the sizes were not equally formed as well as pore shape.

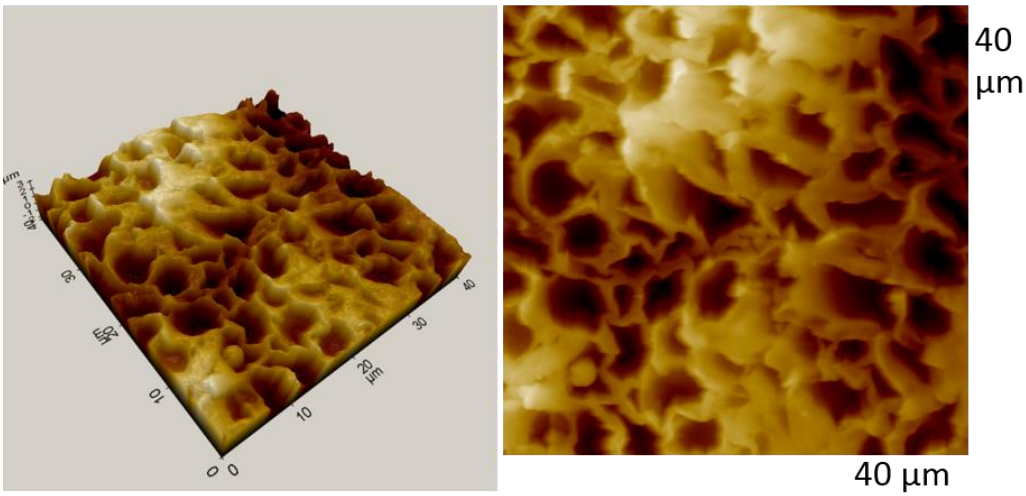

Figure 34 PCL image captured with AFM (Film prepared in THF at concentration 30mg/ml without surfactant)

10.2.4 Effect of humidity in PLA and PCL film properties

The final experiment focused on the humid environment, which can significantly affect the film properties. PLA in ethyl acetate and PCL in THF investigated using different humidity level (56-95%) from film production. In practical way, higher RH% means more condensed fog and higher density of water droplets in the air, which can cause bigger pores on the polymer surface. However, under 56% of relative humidity, pore size increased dramatically in PLA films, which was conflicted with the previous studies. According to the study, it is shown that a relative humidity of 50% is recommend to form the honeycomb film and the pore is regularly increased at higher humidity level [116]. It was assumed that the different regions of the film provided the different structural characteristic because of the non-homogeneous nature of the film. For PCL in THF, it is shown that higher pore size is obtained as humidity increases, namely from 3 µm to 5 µm when humidity increases from 58% to 95% as seen in Figure 35 and in the optical microscopy images shown in Figure 36.

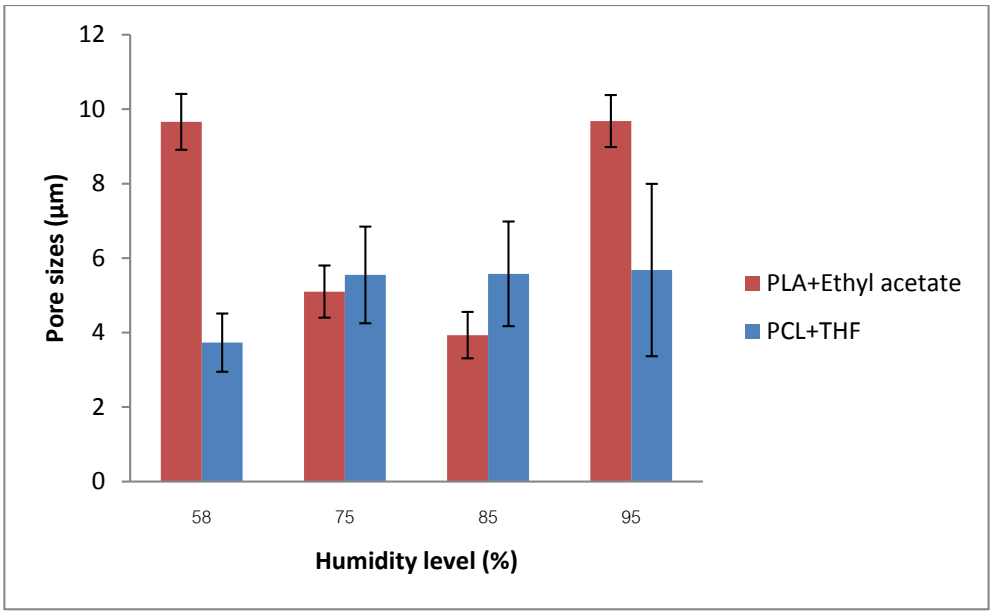

Figure 35 Effect of humidity level in pore size of PLA and PCL films

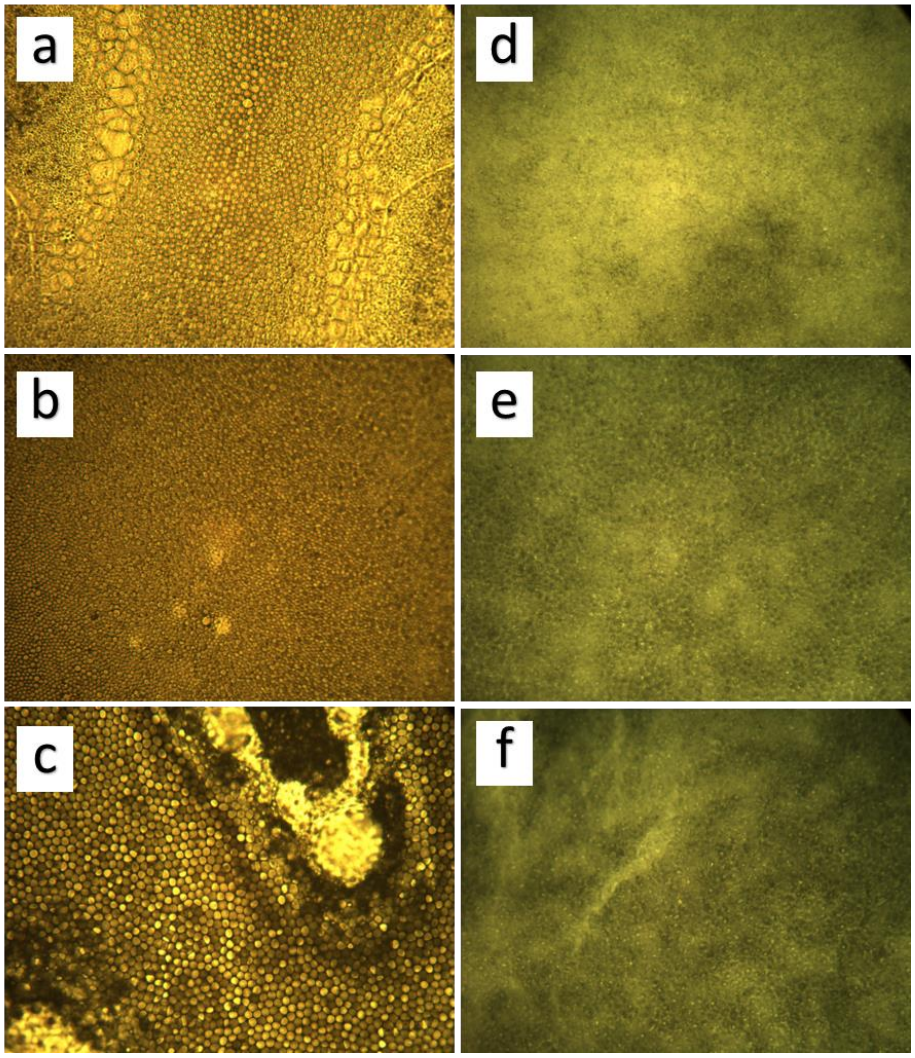

Figure 36 Optical microscopy images taken at 20x magnification a) PLA under 55% of humidity b) PLA under 75-85% of humidity c) PLA under 95% of humidity d) PCL under 55% of humidity e) PLA under 75-85% of humidity f) PLA under 95% of humidity

10.3 Wettability of films

The water contact angle measurement is a common way to check the wettability of the material surface and also the hydrophobic and hydrophilic properties. From Table 6, it can be seen that adding surfactant to the polymer solution generally reduced the water contact angle of the film. For PLA and PCL, Tween 80 provided more hydrophilic surfaces than PVA. Using THF as solvent can dissolve the polymer solution better than ethyl acetate, which can reduce water contact angle as well. The interaction of a liquid drop with a surface depends strongly on the chemistry of the two materials. Polymers dissolved in THF have higher contact angle due to a structure with highly interconnected pores and the polymer can dissolve better than in ethyl acetate, which makse the film even more flat and water droplets were completely distributed on the films. For polymer with surfactant (Figure 37 left), the films pattern with honeycomb array show lower contact angle compared with polymer film without surfactant (Figure 37 right) due to surfactant provides more capability of the polymer solution to form and maintain the pore structure as well as providing more space to create the pores, which were closer one another. According to the study, the contact angle is related to the surface roughness of the material. In this case, the film in the presence of surfactant forming honeycomb pattern increased the surface roughness of the films and, as a result, the contact angle decreased [117].

Table 6 Water contact angle of different parameters of polymer films

Polymer	Solvent	Surfactant	Surfactant concentration	Left angle Ɵ	Right angle Ɵ
PLA	Ethyl acetate	-	-	92.9±11	97.4±12
PLA	Ethyl acetate	Tween 80	0.1%	89±16	89±16
PLA	Ethyl acetate	PVA	5%	109.6±2	111.3±3
PLA	THF	-	-	87±1	87.2±1
PLA	THF	Tween 80	0.1%	35.5±8	33.6±8
PCL	Ethyl acetate	-	-	112±4	114.2±1
PCL	Ethyl acetate	Tween 80	0.1%	83.7±12	81.3±15
PCL	THF	-	-	122.8±3	123.6±2
PCL	THF	Tween 80		100±18	100.8±17

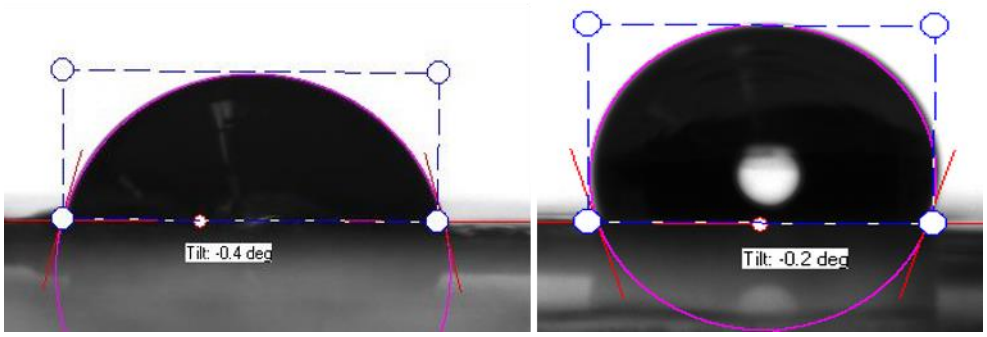

Figure 37 Microscopy images of two types of surface, which contributed to obtain the different water contact angles, left is polymer film with surfactant (Tween 80) and right is the film without surfactant (Tween 80)

10.4 RPE cell culture

For RPE cell culture, there are actually three types of polymer films were tested: PLA in ethyl acetate with Tween 80 and PCL in THF. The images were obtained by fluorescence microscopy, which could reveal actin filaments and nuclei after phalloidin and DAPI staining, respectively. For the first sample (Figure 38a), the cells did not attach properly and were found aggregated after 9 days. For PCL in THF (Figure 38b), the results were better than in the previous case, since the cells spread and covered the entire film. Cell morphology was also in agreement with the typical morphology of RPE cells.

The distribution of actin filaments and nuclei was not uniform in PLA with Tween 80. Moreover, outnumber of pores compared to the surface area is also the factor that the cell cannot grow properly.

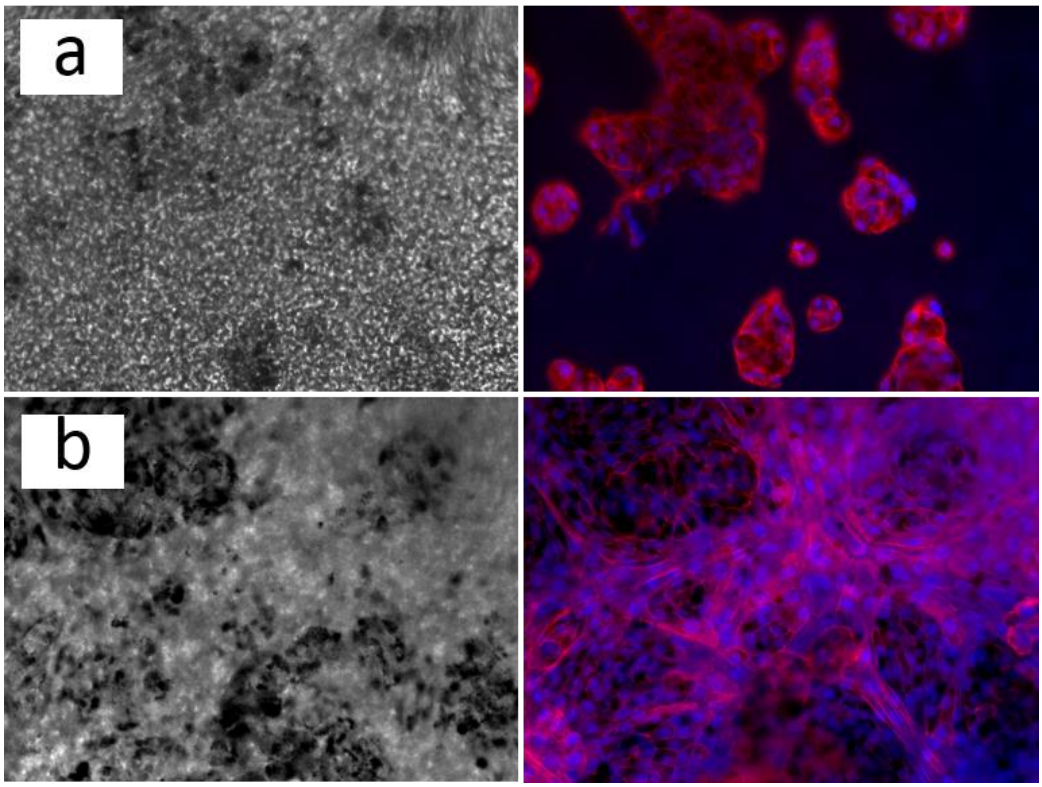

Figure 38 a) PLA in ethyl acetate+Tween 0.1% with RPE cell culture b) PCL+THF with RPE cell culture after 9 days (Left: bright field images; right: fluorescence microscopy images showing the nuclei (blue) and the actin filament (red)).

11. CONCLUSION

The retinal pigment epithelium performs a number of essential roles in the retina such as controlling the amount of minerals or nutrients that nourish the photoreceptors, oxygen absorption and various homeostasis in the ion channels. When using scaffold materials as RPE carries for cell transplantation, pore sizes around 3µm have been considered adequate, since they can allow the free flow of oxygen, nutrients and waste products through the membrane [112].

Different variables of the film production by the BF method such as various kinds of polymers, concentration of polymer/surfactant, solvent and RH%, were studied under humid environment to form a honeycomb pattern on the polymer films. It was concluded that increasing concentration of polymer could reduce pore sizes and increase the film thickness accordingly. If the concentration exceeds more than 30 mg/m, the honeycomb structure was not formed and the pore size tended to increase. For PLA dissolved in ethyl acetate, PLA 26 mg/ml provided the most promising pore size, thickness and contact angle compared to other concentrations. Adding an amphiphilic component or surfactant such as Tween 80 and PVA could change the surface properties of polymers and reduced the pore size as concentration increased. For example, the dried polymer solution became more homogeneous, since the surface tension of the solution was reduced and affected the dissolution of the polymer. Moreover, the surfactant could maintain pore shape and formed the honeycomb pattern on the film with appropriate pore size, pore number and film thickness. However, using high Tween 80 concentration (more than 0.2%) affected the pore shape and could not preserve the honeycomb array on the film. The most suitable surfactant concentration should be controlled around 0.1 %. For PLA in THF, the polymer solution was dissolved in THF better than ethyl acetate, but the honeycomb pattern could not be seen clearly. For PCL films, the type of solvent is the main issue because PCL is relatively difficult to dissolve. In this case, PCL in THF provided more reliable results in the term of pore size, homogeneity of the films and thickness than when using ethyl acetate. PCL solutions prepared in THF at around 30 mg/ml, formed honeycomb films with a pore size of less than 4µm.

The wettability of the films was shown to be related to the pore size. In addition, contact angle decreased when films were prepared in the presence of surfactant compared to films prepared without surfactant because of the roughness on the films.

The final experiment was the RPE cell culture on the polymer films and the observation of cell attachment and cell survivability, which was achieved by my supervisor in BioMediTech TUT/UTA joint biomaterial testing laboratory. Cell attachment worked best on the PCL films in THF without surfactant, in which cells visibly grew and spread throughout the films. On the other hand, PLA in ethyl acetate with Tween 80 as surfactant covers all the structural requirements including pore sizes and honeycomb pattern, but the RPE cells died and became aggregated in some areas, which was unsuccessful. In further studies, the films should be coated with collagen or some substances, which have enough capability for cell attachment on the film especially in PLA films. In addition, the dissolution of the polymers should be improved in order to produce homogeneous films.

REFERENCES

[1] W. Kasai and T. Kondo, "Fabrication of Honeycomb-Patterned Cellulose Films," in *Macromolecular biosensor*, 2003, pp. 17-21.

[2] J. Humphrey and E. Dykesc, "Thermal energy concudction in a honey bee comb due to cell heating Bees," in *J. Theor. Biol.*, 2008, pp. 194-208.

[3] O. Ted M. Montgomery, "Anatomy, Physiology and Pathology of the Human EYE," 15 1 2014. [Online]. Available: http://www.tedmontgomery.com/the_eye/.

[4] T. D. Lamb, "Evolution of the Eye," 16 1 2014. [Online]. Available: http://www.scientificamerican.com/article/evolution-of-the-eye/ .

[5] C. P. Vito RP, "Finite element based mechanical models of the cornea for pressureand indenter loading," *Refractive and Corneal Surgery*, pp. 146-151, 1992.

[6] S. M. Faller A., The human body, 2004.

[7] M. John J. Miller, "About the eye," Georgia Retina, 2014. [Online]. Available: http://www.garetina.com/about-the-eye. [Accessed 14 2 2014].

[8] P. H. Raven and G. B. Johnson, "Sensory system," in *Biology*, McGraw-Hill Science/Engineering/Math, 2000, pp. 1103-1105.

[9] L. TD, C. SP and J. Pugh EN, "Evolution of the vertebrate eye: opsins, photoreceptors, retina and eye cup," in *Nat Rev Neurosci*, 2007.

[10] S. O, "The retinal pigment epithelium in visual function," in *Physiol Rev*, 2005.

[11] D. Hubel, "The eyes," David Hubel's Eye, Brain, and Vision, 2014. [Online]. Available: http://hubel.med.harvard.edu/book/b8.htm. [Accessed 22 1 2014].

[12] M. Jingjing Huang, M. P. Xing Liu, M. Ziqiang Wu, M. Hui Xiao, M. Laurie Dustin and M. Srinivas Sadda, "Macular Thickness Measurements in Normal Eyes with Time Domain and Fourier Domain Optical Coherence Tomography," *PubMed*, vol. 29, no. 7, p. 980–987, 2010.

[13] C. A. Curcio and e. a. K. R. Sloan, "Human photoreceptor topography," in *The Journal of Comparative Neurology 292(4)*, 1990, pp. 497-523.

[14] E. Kandel, J. Schwartz and T. M. Jessell, in *Principles of Neural Science (4th ed.)*, New York, McGraw-Hill, 2000, pp. 507-513.

[15] T. A. Foundation, "Age related macular degeneration," The science of AMD, 2014. [Online]. Available: http://www.scienceofamd.org/learn/. [Accessed 12 6 2014].

[16] B. MM, P. GL and N. TM, "Relative contributions of the neurosensory retina and retinal pigment epithelium to macular hypofluorescence," in *Arch Ophthalmol*, 2000, pp. 27-31.

[17] B. D, "The retinal pigment epithelium: a versatile partner in vision," in *J Cell Sci Suppl*, 1993.

[18] S. RH, "Interactions between the retinal pigment epithelium and the neural retina," in *Doc Ophthalmol* , 1985.

[19] S. JR, H. D and H. CP, "The retinal pigment epithelium in health and disease," in *Curr Mol Med*, 2010.

[20] V. Alder and S. Cringle, "The effect of the retinal circulation on vitreal oxygen tension," in *Current eye research 4*, 1985, pp. 121-129.

[21] M. E. Boulton, "Studying melanin and lipofuscin in RPE cell culture models," *ScienceDirect*, vol. 126, pp. 61-67, 2014.

[22] M. MF, "Clinical electrophysiology of the retinal pigment epithelium," in *Doc Ophthalmol*, 1991.

[23] N. A and M. MF, "Healing of photocoagulation lesions affects the rate of subretinal fluid resorption," in *Ophthalmology*, 1984.

[24] Webvision, "Part II: Anatomy and Physiology of the retina," Webvision The Organization of the Retina and Visual System, 2015. [Online]. Available: http://webvision.med.utah.edu/book/part-ii-anatomy-and-physiology-of-the-retina/. [Accessed 18 1 2015].

[25] R. Sumita, "The fine structure of Bruch's membrane of the human choroid as revealed by electron microscopy," *Journal of Electronmicroscopy*, vol. 10, no. 2, pp. 111-118, 1961.

[26] J. M. Skeie, "Choroidal endothelial cell activation in age-related macular degeneration," in *PhD (Doctor of Philosophy) thesis*, University of Iowa, 2010.

[27] C. A. Curcio and M. Johnson, "Structure, Function, and Pathology of Bruch's Membrane," in *Anatomy and Physiology*, 2010, pp. 465-466.

[28] M. M. John D. Sheppard, "Emedicinehealth," WebMD, Inc, 2015. [Online]. Available: http://www.emedicinehealth.com/macular_degeneration/article_em.htm. [Accessed 8 May 2015].

[29] P. J. Horner and F. H. Gage, "Regenerating the damaged central nervous system," *Macmillan Magazines Ltd*, pp. 963-970, 2000.

[30] D. G. Birch and F. Q. Liang, "Age-related macular degeneration: a target for nanotechnology derived medicines," *PubMed*, vol. 2, no. 1, p. 65–77, 2007.

[31] G. S. Hageman, "Webvision," University of Utah Disclaimer, 2015. [Online]. Available: http://webvision.med.utah.edu/book/part-xii-cell-biology-of-retinal-degenerations/age-related-macular-degeneration-amd/. [Accessed 8 May 2015].

[32] 3. Ferris FL, F. SL and H. L, "Age-related macular degeneration and blindness due to neovascular maculopathy," *Arch Ophthalmol,* vol. 102, pp. 1640-1642, 1984.

[33] M. D. S. staff, "Macular Degeneration Symptoms," Macular Degeneration Symptoms, 2015. [Online]. Available: http://www.maculardegenerationsymptoms.net/. [Accessed 19 1 2015].

[34] P. Gregory S. Hageman, "Age-Related Macular Degeneration (AMD) by Gregory S. Hageman," The Organization of the Retina and Visual System, 2012. [Online]. Available: http://webvision.med.utah.edu/book/part-xii-cell-biology-of-retinal-degenerations/age-related-macular-degeneration-amd/. [Accessed 15 3 2014].

[35] K. A, L. H. E and H. F, "Immunological factors in the pathogenesis and treatment of age-related macular degeneration," in *Ocul Immunol Inflamm*, 2005, pp. 3-11.

[36] J. JB, K. I and D. R, " Intraocular pressure after intravitreal injection," in *Br J Ophthalmol*, 2003.

[37] M. Lylas G. Mogk, "WebMD," WebMD, LLC, 2015. [Online]. Available: http://www.visionaware.org/info/your-eye-condition/age-related-macular-degeneration-amd/treatments-for-dry-macular-degeneration/125. [Accessed 8 May 2015].

[38] L. M. Plum, L. Rink and H. Haase, "The Essential Toxin: Impact of Zinc on Human Health," *NCBI,* vol. 7, no. 4, pp. 1342-1365, 2010.

[39] J. Ophthalmol, "Association of statin use with cataracts: a propensity score-matched analysis," *PubMed,* vol. 131, no. 11, pp. 1427-34, 2013.

[40] M. S. Johanna M. Seddon, "AGE-RELATED MACULAR DEGENERATION (AMD)," New England Eye Center, 1989. [Online]. Available: http://www.neec.com/Pages/Research/ARMD_Study/. [Accessed 20 2 2014].

[41] P. Farinelli, A. Perera, B. Arango-Gonzalez, D. Trifunovic, M. Wagner, T. Carell, M. Biel, E. Zrenner, S. Michalakis, F. Paquet-Durand and P. A. R. Ekström, "DNA methylation and differential gene regulation in photoreceptor cell death," *Cell Death and Disease,* 2014.

[42] K. KOMEIMA, B. S. ROGERS and P. A. CAMPOCHIARO, "Antioxidants Slow Photoreceptor Cell Death in Mouse Models of Retinitis Pigmentosa," *Cellular physiology,* pp. 809-815, 2007.

[43] J. N. Sahni, M. Angi, C. Irigoyen, F. Semeraro, M. R. Romano and F. Parmeggiani, "Therapeutic Challenges to Retinitis Pigmentosa: From Neuroprotection to Gene Therapy," *Curr Genomics,* vol. 12, no. 4, pp. 276-284, 2011.

[44] F. Baino, "The Use of Polymers in the Treatment of Retinal Detachment: Current Trends and Future Perspectives," *MDPI,* pp. 286-322, 2010.

[45] F. Baino, "The Use of Polymers in the Treatment of Retinal Detachment:," *MDPI - Open Access Publishing,* 2010.

[46] H. Witschel and J. Faulborn, "Gewebereaktionen auf Plomben- und Cerclage-material: Polyamid-Silikon-Polyester," in *Graefes Arch. Klin. Exp. Ophthalmol*, 1978, pp. 217-226.

[47] F. Deodati, P. Bec and M. Camezind, "Use of Teflon as an indentation material in retinal detachment surgery," in *Bull. Soc. Ophthalmol. Fr*, 197, pp. 69-71.

[48] B. F., "Scleral buckling biomaterials and implants for retinal detachment surgery," *MEDICAL ENGINEERING & PHYSICS*, vol. 32, pp. 945-956, 2010.

[49] P. Thomsen, O. Omar, G. d. Peppo and K. E. m, " Dental Field and Maxillofacial Area," *JOURNAL OF TISSUE ENGINEERING AND REGENERATIVE MEDICINE*, vol. 6, pp. 1-429, 2012.

[50] C. M. Ramsden, M. B. Powner, A.-J. F. Carr, M. J. K. Smart, L. d. Cruz and P. J. Coffey, "Stem cells in retinal regeneration: past, present and future," *NCBI*, vol. 140, no. 12, p. 2576–2585, 2013.

[51] P. Shu-Zhen Wang and P. Run-Tao Yan, "The Retinal Pigment Epithelium: a Convenient Source of New Photoreceptor cells," *NCBI*, vol. 9, no. 1, pp. 83-93, 2014.

[52] B. A, "Morality and human embryo research. Introduction to the Talking Point on morality and human embryo research," *EMBO reports*, vol. 10, no. 4, pp. 299-300, 2009.

[53] E. Roche, M. M. P. Sepulcre, F. Ensefiat-Waser, J. A. Reig and B. Soria, "Bio-engineering insulin-secreting cellsfrom embryonic stem cells: a review of progress," *Med. Biol. Eng. Comput*, vol. 41, 2003.

[54] C. I. Falkner-Radler, I. Krebs, C. Glittenberg, B. Považay, W. Drexler, A. Graf and S. Binder, "Outcome After Autologous RPE-choroid Sheet and RPE Cell-suspension in a Randomised Clinical Study," *The British Journal of Ophthalmology*, vol. 95, no. 3, p. 431, 2011.

[55] Y. Huang, V. Enzmann and S. T. Ildstad, "Stem cell-based therapeutic applications in retinal degenerative diseases," *NCBI*, vol. 7, no. 2, pp. 434-445, 2011.

[56] S. Becker, H. Jayaram and G. A. Limb, "Recent Advances towards the Clinical Application of Stem Cells for Retinal Regeneration," *Cells*, vol. 1, pp. 851-873, 2012.

[57] M. Mark B. Abelson and J. McLaughlin, "The use of stem cells may greatly increase the success rate of transplants," *Review of ophthalmology*, 2007.

[58] S. R. Montezuma, J. Loewenstein, C. Scholz and I. Joseph F. Rizzo, "Biocompatibility of Materials Implanted into the Subretinal Space of Yucatan Pigs," *Investigative Ophthalmology & Visual Science*, vol. 47, pp. 3514-3522, 2006.

[59] M. Trese, C. V. Regatieri and M. J. Young, "Advances in Retinal Tissue Engineering," *MDPI*, vol. 5, pp. 108-120, 2012.

[60] A. SCHNERCH, C. CERDAN and M. BHATIA, "Distinguishing Between Mouse and Human Pluripotent Stem Cell Regulation: The Best Laid Plans of Mice and Men," *Stem cells,* vol. 28, no. 3, pp. 419-430, 210.

[61] T. JA, I.-E. J, S. SS, W. MA, S. JJ and Marshall, "Embryonic stem cell lines derived from human blastocysts," *Science 282,* pp. 1145-1147, 1998.

[62] C. Allegrucci and L. Young, "Differences between human embryonic stem cell lines," *Oxford Journals,* vol. 13, no. 2, pp. 103-120, 2007.

[63] 1. H. Ö. M. H. Julien Barthes, A. Ndreu-Halili, A. Hasan and N. E. Vrana, "Cell Microenvironment Engineering and Monitoring for Tissue Engineering and Regenerative Medicine: The Recent Advances," *BioMed Research International,* p. 18, 2014.

[64] P. Gilbert, K. Havenstrite, K. Magnusson, A. Sacco, 5. P. K. NA Leonardi, N. Nguyen, S. Thrun, M. Lutolf and H. Blau, "Substrate elasticity regulates skeletal muscle stem cell self-renewal in culture," *NCBI,* vol. 329, no. 5995, pp. 1078-1081, 2011.

[65] S. Baiguera, L. Urbani and C. D. Gaudio, "Tissue Engineered Scaffolds for an Effective Healing and Regeneration: Reviewing Orthotopic Studies," *BioMed Research International,* p. 27, 2014.

[66] K. S. W. Sing, D. H. Everett, R. A. W. Haul, L. Moscou, R. A. Pierotti, J. Rouquerol and T. Siemieniewska, " Reporting Physisorption Data For Gas/Solid Systems with Special Reference to the Determination of Surface Area and Porosity," in *Pure Appl. Chem,* 1985, pp. 603-619.

[67] S. P. Adiga, C. Jin, L. A. Curtiss, N. A. Monteiro-Riviere and R. J. Narayan, "Nanoporous membranes for medical and biological applications," in *John Wiley & Sons Inc.*, 2009, pp. 568-581.

[68] T. n. p. t. f.-b. d. d. systems, "Wei Yan; Vincent K.S. Hsiao; Yue Bing Zheng; Yasir M. Shariff; Tieyu Gao; Tony Jun Huang," *ScienceDirect,* vol. 517, pp. 1794-1798, 2009.

[69] R. Langer, "Biomaterials in drug delivery and tissue engineering: one laboratory's experience," *Acc. Chem. Res,* vol. 33, pp. 94-101, 2000.

[70] G. Giordano, R. Thomson, S. Ishaug, A. Mikos, S. Cumber, C. Garcia and D. Lahiri-Munir, "Retinal pigment epithelium cells cultured on synthetic biodegradable polymers," in *J. Biomed. Mater. Res*, 1997, pp. 87-93.

[71] R. Langer and J. Vacanti, Tissue engineering. Science, 1993.

[72] J. Humphrey and E. Dykesc, "Thermal energy conduction in a honey bee comb due to cells-heating Bees," in *J. Theor. Biol,* 2008, pp. 194-208.

[73] S. Kamat, X. Su, R. Ballarini and A. Heuer, "Structural basis for the fracture toughness of the shell of the conch strombus giggas," in *Nature,* 2000, p. 1036–1040.

[74] G. Widawski, M. Rawiso and B. Francois, "Self-organized honeycomb morphology of star-polymer polystyrene films," in *Nature*, 1994, pp. 387-389.

[75] K. Zhang, H. Duan, B. Karihaloo and J. Wang, "Hierarchical, multilayered cell walls reinforced by recycled silk cocoons enhance the structural integrity of honeybee combs," in *Proc. Natl. Acad. Sci. USA*, 2010, p. 9502–9506.

[76] D. H. Bai, C. Du, A. Zhang and P. L. Li, "Breath Figure Arrays: Unconventional Fabrications, Functionalizations, and Applications," in *Angewandte Chemie International Edition*, 2013, p. 12240–12255.

[77] W. G, R. M and F. B, Nature, 1994.

[78] A. Saunders, J. Dickson, P. Shah, M. Lee, K. Lim, K. Johnston and B. Korgel, "Breath figure templated self-assembly of porous diblock," in *Physical Review E, vol. 73*, 2006, pp. 1-7.

[79] U. Bunz, "Breath figures as a dynamic templating method for polymers and nanomaterials.," in *Adv. Mater*, 2006, pp. 973-989.

[80] M. Stenzel-Rosenbaum, T. Davis, A. Fane and V. Chen, "Porous polymer films and honeycomb structures made by the self-organization of well-defined macromolecular structures created by living radical polymerization techniques," in *Angew. Chem. Int. Ed. Engl*, 2001, p. 3428–3432.

[81] C. Barner-Kowollik, H. Dalton, T. Davis and M. Stenzel, "Nano- and micro-engineering of ordered porous blue-light-emitting films by templating well-defined organic polymers around condensing water droplets," in *Angew.Chem. Int. Ed. Engl*, 2003, p. 3664–3668.

[82] L. Lu and S. Jenekhe, "Poly(vinyl diphenylquinoline): A new pH-tunable light-emitting and charge-transport polymer synthesized by a simple modification of polystyrene," in *Macromolecules*, 2001, p. 6249–6254.

[83] M. Stenzel, T. Davis and A. Fane, "Honeycomb structured porous films prepared from carbohydrate based polymers synthesized via the RAFT process," in *J. Mater. Chem*, 2003, p. 2090–2097.

[84] N. Park, M. Seo and S. Kim, "Particle and breath figure formation of triblock copolymers having self-complementary hydrogen-bonding units," in *J. Polym. Sci. Part A Polym. Chem*, 2012, p. 4408–4414.

[85] J. Kadla, F. Asfour and B. Bar-Nir, "Micropatterned thin film honeycomb materials from regiospecifically modified cellulose," in *Biomacromolecules*, 2007, pp. 161-165.

[86] Y. Fukuhira, E. Kitazono, T. Hayashi, H. Kaneko, M. S. M. Tanaka and Y. Sumi, "Biodegradable honeycomb-patterned film composed of poly(lactic acid) and dioleoylphosphatidylethanolamine," in *Biomaterials*, 2006, p. 1797–1802.

[87] E. Nomura, A. Hosoda, M. Takagaki, H. Mori, Y. Miyake, M. Shibakami and H. Taniguchi, "Self-organized honeycomb-patterned microporous polystyrene thin

films fabricated by calix[4]arene derivatives," in *Langmuir*, 2010, p. 10266–10270.

[88] D. V. Zagorevskii, M. J. Nasrullah, V. Raghunadh and B. C. Benicewicz, "The effect of tetrahydrofuran as solvent on matrix-assisted laser desorption/ionization and electrospray ionization mass spectra of functional polystyrenes," *RAPID COMMUNICATIONS IN MASS SPECTROMETRY,* vol. 20, pp. 178-180, 2006.

[89] D. Lide, Handbook of chemistry and physics (80th ed.)CRC Press, Boca Raton, 1999.

[90] S. Lower, "Chem1 General Chemistry Virtual Textbook," Chem1, 2009. [Online]. Available: http://www.chem1.com/acad/webtext/states/liquids.html. [Accessed 2015 2 6].

[91] G. A. Ruffo, Geometrical features induced in polymer structures by self-assembly and their exploitation for biomedical use, 2011.

[92] S. Hynes and E. Lavik, "A tissue-engineered approach towards retinal repair: scaffolds for cell transplantation to the subretinal space," in *Graefes Arch. Clin. Exp. Ophthalmol,* 2010, pp. 763-778.

[93] H. Sunami, E. Ito, M. Tanaka, S. Yamamoto and M. Shimomura, "Effect of honeycomb film on protein adsorption, cell adhesion and proliferation," in *Colloids and Surfaces. A, Physicochemical and Engineering Aspects*, 2006, pp. 548-551.

[94] A. Tsuruma, T. Masaru, S.-a. Yamamoto and M. Shimomura, "Suppression of Neural Stem Cell Differentiation by Honeycomb-Patterned Films," *IFMBE Proceedings,* vol. 14, pp. 3558-3561, 2007.

[95] W. X and W. S, "Regulating MC3T3-E1 cells on deformable poly(ε-caprolactone) honeycomb films prepared using a surfactant-free breath figure method in a water-miscible solvent," *PubMed,* vol. 4, no. 9, pp. 4966-75, 2012.

[96] J. B. Chaudhuri, M. G. Davidson, M. J. Ellis, M. D. Jones and X. Wu, "Fabrication of Honeycomb-Structured Poly(DL-lactide) and Poly[(DL-lactide)-co-glycolide)] Films and their Use as Scaffolds for Osteoblast-Like Cell Culture," in *Macromolecular Symposia*, 2008, pp. 52-57.

[97] F. S, P. M, F. P, G. L, F. T, P. CP and Z. V, "Patterned poly(lactic acid) films support growth and spontaneous multilineage gene expression of adipose-derived stem cells," *PubMed,* vol. 93, pp. 92-9, 2012.

[98] Y. Fukuhira, E. Kitazonoa, T. Hayashia, H. Kanekoa, M. Tanakab, M. Shimomura and Y. Sumi, "Biodegradable honeycomb-patterned film composed of poly(lactic acid) and dioleoylphosphatidylethanolamine," *PubMed,* vol. 27, no. 9, p. 1797–1802, 2006.

[99] M. Tanakaa, K. Nishikawa, H. Okubod, H. Kamachid, T. Kawaid, M. Matsushita, S. Todob and M. Shimomura, "Control of hepatocyte adhesion and function on

self-organized honeycomb-patterned polymer film," *ScienceDirect,* Vols. 284-285, p. 464–469, 2006.

[100] X. Wu, M. D. Jones, M. G. Davidson, J. B. Chaudhuri and M. J. Ellis, "Surfactant-free poly(lactide-co-glycolide) honeycomb films for tissue engineering: relating solvent, monomer ratio and humidity to scaffold structure," in *Regenerative Medicine and Biomaterials*, 2008.

[101] T. Nishikawa, R. Ookura, J. Nishida, T. Sawadaishi and M. Shimomura, "Honeycomb film of an amphiphilic copolymer: Fabrication and characterization," *RIKEN Review,* vol. 37, 2001.

[102] W. Kasai and T. Kondo, "Fabrication of Honeycomb-Patterned Cellulose Films," in *Macromolecular Bioscience*, 2003, pp. 17-21.

[103] K. Lang, D. A. Hite, R. W. Simmonds, R. McDermott, D. P. Pappas and J. M. Martinis, "Conducting atomic force microscopy for nanoscale tunnel barrier characterization," in *Review of Scientific Instruments*, 2004, p. 2726–2731.

[104] B. Cappella and G. Dietler, "Force-distance curves by atomic force microscopy," in *Surface Science Reports*, 1999, p. 1–104.

[105] G. Binnig, C. F. Quate and C. Gerber, "Atomic Force Microscope," in *Physical Review Letters*, 930–933, p. 1986.

[106] J. A. Kidd, "University of Virginia school of medicine," Rector and Board of Visitors, 2015. [Online]. Available: http://pharm.virginia.edu/facilities/atomic-force-microscope-afm/. [Accessed 26 1 2015].

[107] A. Adamson and G. A.P., Physical Chemistry of Surfaces. 6th ed, NewYork: ohn Wiley & Sons, 1997.

[108] R. Gould, Contact angle wettability and adhesion American Chemical Society, 1964.

[109] W. Zisman, "F. Fowkes, ed. Contact Angle," in *Wettability, and Adhesion*, 1964, pp. 1-51.

[110] V. e. al, "Toward the defined and xeno-free differentiation of functional human pluripotent stem cell-derived retinal pigment epithelial cells," *Molecular Vision,* vol. 17, pp. 558-575, 2011.

[111] M. H. STENZEL, C. BARNER-KOWOLLIK and T. P. DAVIS, "Formation of Honeycomb-Structured, Porous Films via Breath Figures with Different Polymer Architectures," *Wiley InterScience,* 2006.

[112] A. VA and C. SJ, "The effect of the retinal circulation on vitreal oxygen tension," *PubMed,* vol. 4, no. 2, pp. 121-9, 1985.

[113] R. O. J. N. T. S. M. S. Takehiro Nishikawa, "Honeycomb film of an amphiphilic copolymer: Fabrication and characterization," *Focused on Nanotechnology in RIKEN,* no. 37, 2001.

[114] H. Bai, C. Du, A. Zhang and L. Li, "Breath Figure Arrays: Unconventional Fabrications, Functionalizations, and Applications," in *Angewandte Chemie International Edition*, 2013, p. 12240–12255.

[115] M. McCann, "HEALTH HAZARDS OF SOLVENTS," in *Health and Safety in the Arts Library*, New York NY, 1994.

[116] M. H. STENZEL, C. BARNER-KOWOLLIK and T. P. DAVIS, "Formation of Honeycomb-Structured, Porous Films via Breath Figures with Different Polymer Architectures," *Wiley InterScience*, 2006.

[117] L. Heng, R. Hu, S. Chen, J. Li, L. Jiang and B. Z. Tang, "Patterned Honeycomb Structural Films with Fluorescent and Hydrophobic Properties," *Nanomaterials*, p. 8, 2013.

[118]

[119] S. Priyadarshini, "Eye: Structure, Working and Defects," Biology discussion, [Online]. Available: http://www.biologydiscussion.com/essay/essay-on-eye-structure-working-and-defects/4979. [Accessed 18 1 2014].

[120] A. F. PhD, "Extraocular Muscles: anatomy and clinical investigation-Binocular vision," Optometry, 2010. [Online]. Available: http://www.optometry.co.uk/uploads/articles/CET%20020710%20(2).pdf. [Accessed 18 1 2014].

[121] R. Cicala, "The Camera Versus the Human Eye," Petapixel, 17 11 2012. [Online]. Available: http://petapixel.com/2012/11/17/the-camera-versus-the-human-eye/. [Accessed 20 1 2014].

[122] M. P. Rand Swenson, "Basic human anatomy," in *The eye*, 2008, p. Chapter 46.

[123] B. Cassin and S. Solomon, "Dictionary of eye terminology," in *Gainesville, Fla*, ISBN 0-937404-33-0, 1990.

[124] S. JW and N. JY, "Induction of anterior chamber-associated immune deviation requires an intact, functional spleen," *J Exp Med*, vol. 153, no. 5, p. 1058–1067, 1981.

[125] J. Stein-Streilein, "Research Story Eye and Ear," Schepens Eye Research Institute, 2014. [Online]. Available: http://www.schepens.harvard.edu/research-storystein/joan-stein-streilein-phd/research-story.html. [Accessed 22 1 2014].

[126] F. J. Goes, "Anatomy of Human eye," in *The Eye in History*, 2013, p. 15.

[127] F. Netter, Atlas of Human Anatomy, 2011.

[128] R.-E. Paul, "Anatomy & Embryology of the Eye," in *Vaughan & Asbury's General Ophthalmology (17th ed.)*, 2008.

[129] B. P. Danysh and M. K. Duncan, "The Lens Capsule," *PubMed*, vol. II, no. 88, p. 151–164, 2009.

[130] A. S. B.-. Giampani and J. G. Junior, Anatomy of Ciliary Body, Ciliary Processes, 2013.

[131] M. Yanoff and J. S. Duker, "Anatomy of the Uvea," in *Ophthalmology*, 2004, p. 775.

[132] P. Marianne Price, "How the Human Eye Works: A Gateway to Vision," Cornea Research foundation of America, 2014. [Online]. Available: http://www.cornea.org/index.php/hope/how_eye_works. [Accessed 2 2 2014].

[133] L. Williams and Wilkins, "Eyes," in *NURSING ASSESSMENT OF PHYSICAL SYSTEMS*, 2004, pp. 228-230.

[134] Martini and F. E. Al, Anatomy and Physiology, 2007, pp. 416-426.

[135] L. B. Arey, "Developmental Anatomy," in *A Textbook and Laboratory Manual ofEmbryology. 7th ed*, 1965, pp. 529-541.

[136] A. N. H. H. Hopper, The sense organs In: Foundations of Animal Development. 2nd ed, 1985, pp. 523-545.

[137] L. LUNDSTRÖM, "Wavefront Aberrations," *Royal Institute of Technology*, p. 3, 2007.

[138] T. Almubrad and S. Akhtar, "Structure of corneal layers, collagen fibrils, and proteoglycans of," *Molecular Vision*, no. 17, pp. 2283-2291, 2011.

[139] V. RP and C. PH, "Finite element based mechanical models of the cornea for pressure," in *Refractive and Corneal Surgery*, 1992, pp. 146-151.

[140] K. LT, K. N, O. S and U. E, "Numerical prediction of airbag caused," in *SAE International Congress and Exposition,*, MI, 1998.

[141] thebrain, "PHOTORECEPTORS," The brain from top to bottom, 2014. [Online]. Available: http://thebrain.mcgill.ca/flash/d/d_02/d_02_m/d_02_m_vis/d_02_m_vis.html. [Accessed 20 1 2014].

[142] J. D. Reynolds and S. E. Olitsky, "Anatomy and Physiology of retina," in *Pediatric Retina*, 2011, p. 40.

[143] C. Oyster, " Retinal III: regional variation and spatial organization," in *Oyster, C. (ed.) The Human Eye – Structure and Function*, Sunderland, Massachusetts, Sinauer Associates, 1999, pp. 649-700.

[144] P. Valentin Dragoi, "Visual Processing: Eye and Retina," in *Neurosciene Sensory System*, 1997.

[145] C. R. Center, "MyClearVision," Refractec, Inc, 2015. [Online]. Available: http://www.myclearvision.com/210.asp?nav=200. [Accessed 19 1 2015].

[146] M. C. Staff, "Mayo Clinic," Mayo Foundation for Medical Education and Research, 2012. [Online]. Available: http://www.mayoclinic.org/diseases-conditions/nearsightedness/basics/definition/con-20027548. [Accessed 19 1 2015].

[147] I. Michaelson, "Disturbance of the chorio-capillaris and retinal dehiscence," in *Br. J. Ophthalmol*, 1954, pp. 632-633.

[148] B. J. Anderson and H. McIntosh, "Retinal circulation," in *Annu. Rev. Med*, 1967, pp. 15-26.

[149] H. Taylor, S. West, B. Munoz, F. Rosenthal, S. Bressler and N. Bressler, The long-term effects of visible light on the eye, 1992.

[150] S. H, S. AM, M. E, I. J, H. O and a. L. R, "Unique gene expression signature by human embryonic stem cells cultured," in *Stem Cells*, 2006.

[151] I. Y. C. L. Klimanskaya, J. Meisner, M. W. Johnson and R. Lanza, "Human embryonic stem cells derived without feeder cells," *PubMed,* p. 1636–1641, 2005.

[152] K. A. Ludwig, D. S. Kelley, D. A. Butterfield, B. K. Nelson and G. Fru-Green, "Formation and evolution of carbonate chimneys," *Science Direct*, p. 3625–3645, 2006.

[153] Z. S. L. W. W. X. N. S. D. X. Jingyi Gong1, G. Shui, H. Yang, R. G. Parton and P. Li, "Fsp27 promotes lipid droplet growth by lipid exchange and transfer at lipid droplet contact sites," *JCB*, vol. 195, no. 6, pp. 953-963, 2011.

[154] L. Heng, B. Wang, M. Li, Y. Zhang and L. Jiang, "Advances in Fabrication Materials of Honeycomb Structure Films by the Breath-Figure Method," *PubMed,* 2012.

[155] T. JA, I.-E. J, S. SS, W. MA, S. JJ, M. VS and J. JM, "Embryonic stem cell lines derived from human blastocysts," *PubMed,* vol. 282, no. 5391, pp. 1145-7, 1998.

[156] J. Wang and L. Ye, "Structure and properties of hydrophobic cationic poly(vinyl alcohol)," in *Polymer International*, 2011, pp. 571-580.

[157] M. Franklin W. Lusby and L. V. Institute, "MedlinePlus," U.S. National Library of Medicine, 2 September 2014. [Online]. Available: http://www.nlm.nih.gov/medlineplus/ency/article/001017.htm. [Accessed 8 May 2015].

[158] P. Jeffrey W. Ruberti, P. Abhijit Sinha Roy and P. Cynthia J. Roberts, "CORNEAL STRUCTURE AND FUNCTION," in *Corneal Biomechanics and Biomaterials* , 2011, pp. 269-295.

[159] J. Assawachananont, M. Mandai, S. Okamoto, C. Yamada, M. Eiraku, S. Yonemura, Y. Sasai and M. Takahashi, "Transplantation of Embryonic and Induced Pluripotent Stem Cell-Derived 3D Retinal Sheets into Retinal Degenerative Mice," *NCBI,* vol. 2, no. 5, pp. 662-674, 2014.